

1 **Simulating human impacts on global water resources using**
2 **VIC-5**

3 Bram Droppers¹, Wietse H.P. Franssen¹, Michelle T.H. van Vliet², Bart Nijssen³, Fulco
4 Ludwig¹

5 ¹ Water Systems and Global Change Group, Department of Environmental Sciences, Wageningen
6 University, Wageningen, 6708 PB, The Netherlands

7 ² Department of Physical Geography, Utrecht University, Utrecht, 3584 CS, The Netherlands

8 ³ Computational Hydrology Group, Department of Civil and Environmental Engineering, University of
9 Washington, Seattle, 98195, United States of America

10 *Correspondence to:* Bram Droppers (bram.droppers@wur.nl)

11 **Abstract.** Questions related to historical and future water resources and scarcity have been addressed
12 by several macro-scale hydrological models. One of these models is the Variable Infiltration Capacity
13 (VIC) model. However, further model developments were needed to holistically assess anthropogenic
14 impacts on global water resources using VIC.

15 Our study developed VIC-WUR, which extends the VIC model with: (1) integrated routing, (2) surface
16 and groundwater use for various sectors (irrigation, domestic, industrial, energy and livestock), (3)
17 environmental flow requirements for both surface and groundwater systems, and (4) dam operation.
18 Global gridded datasets on sectoral demands were developed separately and used as an input to the VIC-
19 WUR model.

20 Simulated national water withdrawals were in line with reported FAO national annual withdrawals (R^2
21 adjusted > 0.8), both per sector as well as per source. However, trends in time for domestic and industrial
22 water withdrawal were mixed compared to other previous studies. GRACE monthly terrestrial water
23 storage anomalies were well represented (global mean RMSE of 1.9 and 3.5 for annual and interannual
24 anomalies respectively), while groundwater depletion trends were overestimated. The implemented
25 human impact modules increased simulated streamflow performance for 370 out of 462 human-
26 impacted GRDC monitoring stations, mostly due to the effects of reservoir operation. An assessment of
27 environmental flow requirements indicates that global water withdrawals have to be severely limited
28 (by 39 %) to protect aquatic ecosystems, especially for groundwater withdrawals.

29 VIC-WUR has potential for studying impacts of climate change and anthropogenic developments on
30 current and future water resources and sectoral specific-water scarcity. The additions presented here
31 make the VIC model more suited for fully-integrated worldwide water-resource assessments and
32 substantially decrease computation times compared to previous versions.

33 **1 Introduction**

34 Questions related to historical and future water resources and scarcity have been addressed by several
35 macro-scale hydrological models over the last few decades (Liang et al., 1994; Alcamo et al., 1997;
36 Hagemann and Gates, 2001; Takata et al., 2003; Krinner et al., 2005; Bondeau et al., 2007; Hanasaki et
37 al., 2008a; Van Beek and Bierkens, 2008; Best et al., 2011). Early efforts focussed on the simulation of
38 natural water resources and the impacts of land cover and climate change on water availability (Oki et
39 al., 1995; Nijssen et al., 2001a; Nijssen et al., 2001b). Recently, a larger focus has been on incorporating
40 anthropogenic impacts, such as water withdrawals and dam operations, into water resource assessments
41 (Alcamo et al., 2003; Haddeland et al., 2006b; Biemans et al., 2011; Wada et al., 2011b; Hanasaki et al.,
42 2018).

43 Global water withdrawals increased eight-fold over the last century and are projected to increase further
44 (Shiklomanov, 2000; Wada et al., 2011a). Although water withdrawals are only a small fraction of the
45 total global runoff (Oki and Kanae, 2006), water scarcity can be severe due to the variability of water in
46 both time and space (Postel et al., 1996). Already severe water scarcity is experienced by two-thirds of
47 the global population for at least part of the year (Mekonnen and Hoekstra, 2016). To stabilize water
48 availability for different sectors (e.g. irrigation, hydropower, and domestic uses) dams and reservoirs
49 were built, which are able to strongly affect global river streamflow (Nilsson et al., 2005; Grill et al.,
50 2019). In addition, groundwater resources are being extensively exploited to meet increasing water
51 demands (Rodell et al., 2009; Famiglietti, 2014).

52 One of widely-used macro-scale hydrological models is the Variable Infiltration Capacity (VIC) model.
53 The model was originally developed as a land-surface model (Liang et al., 1994), but has been mostly
54 used as a stand-alone hydrological model (Abdulla et al., 1996; Nijssen et al., 1997) using an offline
55 routing module (Lohmann et al., 1996; Lohmann et al., 1998a, b). Where land-surface models focus on
56 the vertical exchange of water and energy between the land surface and the atmosphere, hydrological
57 models focus on the lateral movement and availability of water. By combining these two approaches,
58 VIC simulations are strongly process-based and this, in turn, provides a good basis for climate-impact
59 modelling.

60 VIC has been used extensively in studies ranging from: coupled regional climate model simulations
61 (Zhu et al., 2009; Hamman et al., 2016), combined river streamflow and water-temperature simulations
62 (van Vliet et al., 2016), hydrological sensitivity to climate change (Hamlet and Lettenmaier, 1999;
63 Nijssen et al., 2001a; Chegwiddden et al., 2019), global streamflow simulations (Nijssen et al., 2001b),
64 sensitivity in flow regulation and redistribution (Voisin et al., 2018; Zhou et al., 2018), and real-time
65 drought forecasting (Wood and Lettenmaier, 2006; Mo, 2008). Several studies used VIC to simulate the
66 anthropogenic impacts of irrigation and dam operation on water resources (Haddeland et al., 2006a;
67 Haddeland et al., 2006b; Zhou et al., 2015; Zhou et al., 2016) based on the model setup of Haddeland et
68 al. (2006b). However, further developments were needed to holistically assess anthropogenic impacts
69 on global water resources using VIC (Nazemi and Wheeler, 2015a, b; Döll et al., 2016; Pokhrel et al.,
70 2016).

71 Firstly, the VIC model did not yet include groundwater withdrawals or water withdrawals from
72 domestic, manufacturing and energy (thermoelectric) sources. Although these sectors use less water than
73 irrigation (Shiklomanov, 2000; Grobicki et al., 2005; Hejazi et al., 2014) they are locally important
74 actors (Gleick et al., 2013), especially for the water-food-energy nexus (Bazilian et al., 2011). Sufficient
75 water supply and availability are essential for meeting a range of local and global sustainable
76 development goals related to water, food, energy and ecosystems (Bijl et al., 2018). Secondly,
77 environmental flow requirements (EFRs) were often neglected (Pastor et al., 2014), even though they
78 are “necessary to sustain aquatic ecosystems which, in turn, support human cultures, economies,
79 sustainable livelihoods, and well-being” (Brisbane Declaration, 2017). Anthropogenic alterations
80 already strongly affect freshwater ecosystems (Carpenter et al., 2011), with more than a quarter of all
81 global rivers experiencing very high biodiversity threats (Vorosmarty et al., 2010). By neglecting EFRs,
82 sustainable water availability for anthropogenic uses is overestimated (Gerten et al., 2013). Lastly, while
83 the model setup of Haddeland et al. (2006b) already included important anthropogenic impact modules
84 (i.e. irrigation and dam operation), these were not fully integrated yet. Therefore multiple successive
85 model runs were required which was computationally expensive, especially for global water resources
86 assessments.

87 Recently version 5 of the VIC model (VIC-5) was released (Hamman et al., 2018), which focussed on
88 improving the VIC model infrastructure. These improvements provide the opportunity to fully integrate
89 human-impacts into the VIC model framework, while reducing computation times. Here the newly
90 developed VIC-WUR model is presented (named after the developing team at Wageningen University
91 and Research). The VIC-WUR model extends the existing VIC-5 model with several modules that
92 simulate the anthropogenic impacts on water resources. These modules will implement previous major
93 works on anthropogenic impact modelling as well as integrate environmental flow requirements into
94 VIC-5. The modules include: (1) integrated routing, (2) surface and groundwater use for various sectors
95 (irrigation, domestic, industrial, energy and livestock), (3) environmental flow requirements for both
96 surface and groundwater systems, and (4) dam operation.

97 The next section first describes the original VIC-5 hydrological model (Section 2.1), which calculates
98 natural water resource availability. Subsequently the integration of the anthropogenic impact modules,
99 which modify the water resource availability, are described (Section 2.2). Global anthropogenic water
100 uses for each sector are also estimated (Section 2.3). To assess the capability of the newly developed
101 modules, the VIC-WUR results were compared with FAO national water withdrawals by sector and by
102 source (FAO, 2016); Huang et al. (2018), Steinfeld et al. (2006), and Shiklomanov (2000) data on water
103 withdrawals by sector; GRACE terrestrial water storage anomalies (NASA, 2002); GRDC streamflow
104 timeseries (GRDC, 2003); and Yassin et al. (2019) and Hanasaki et al. (2006) data on reservoir operation
105 (Section 3.2). VIC-WUR simulations results are also compared with various other state-of-the-art global
106 hydrological models. Lastly, the impacts of adhering to surface and groundwater environmental flow
107 requirements on water availability are assessed (Section 3.3). This assessment is included to indicate the
108 effects of the newly integrated surface and groundwater environmental flow requirements on worldwide
109 water availability.

110 **2 Model development**

111 **2.1 VIC hydrological model**

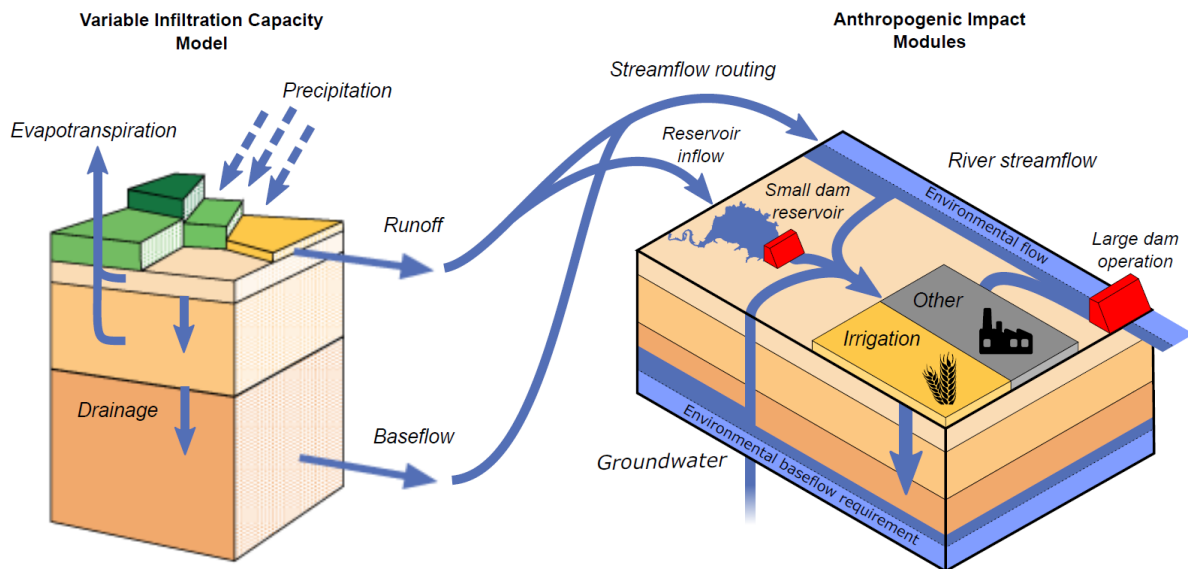
112 The basis of the VIC-WUR model is the Variable Infiltration Capacity model version 5 (VIC-5) (Liang
113 et al., 1994; Hamman et al., 2018). VIC-5 is an open source macro-scale hydrological model that
114 simulates the full water and energy balance on a (latitude – longitude) grid. Each grid cell accounts for
115 sub-grid variability in land cover and topography, and allows for variable saturation across the grid cell.
116 For each sub-grid the water and energy balance is computed individually (i.e. sub-grid do not exchange
117 water or energy between one another). The methods used to calculate the water and energy balance are
118 summarized in Appendix A, mainly based on the work of Liang et al. (1994). For the description of the
119 global calibration and validation of the water balance one is referred to Nijssen et al. (2001b).

120 VIC version 5 (Hamman et al., 2018) upgrades did not change the model representation of physical
121 processes, but improved the model infrastructure. Improvements include the use of NetCDF for
122 input/output and the implementation of parallelization through Message Passing Interface (MPI). These
123 changes increase computational speed and make VIC-5 better suited for (computationally expensive)
124 global simulations. The most significant modification that enables new model applications is that VIC-
125 5 also changed the processing order of the model. In previous versions all timesteps were processed for
126 a single grid cell before continuing to the next cell (time-before-space). In VIC-5 all grid cells are
127 processed before continuing to the next timestep (space-before-time). This development allows for
128 interaction between grid cells every timestep, which is important for full integration of the anthropogenic
129 impact modules, especially water withdrawals and dam operation.

130 For example, surface and subsurface runoff routing to produce river streamflow was typically done as a
131 post-process operation (Lohmann et al., 1996; Hamman et al., 2017), due to the time-before-space
132 processing order of previous versions. Therefore, water withdrawals could not be taken into account
133 directly and studies using the model setup of Haddeland et al. (2006b) required multiple successive
134 model runs. Since VIC-5 uses the space-before-time processing order, runoff routing could be simulated
135 each timestep. The routing post-process was replaced by our newly developed routing module which
136 simulates routing sequentially (upstream-to-downstream) to facilitate water withdrawals between cells.

137 **2.2 Anthropogenic-impact modules**

138 VIC-WUR extends the existing VIC-5 though the addition of several newly developed anthropogenic-
139 impact modules (Figure 1). These modules include sector-specific water withdrawal and consumption,
140 environmental flow requirements for both surface and groundwater systems and dam operation for large
141 and small (within-grid) dams.



142

143 **Figure 1: Schematic overview of the VIC-WUR model that includes the VIC-5 model and several anthropogenic impact**
144 **modules. Water from river streamflow, groundwater and small (within-grid) reservoirs are available for withdrawal.**
145 **Surface and groundwater withdrawals are constrained by environmental flow requirements. Withdrawn water is**
146 **available for irrigation, domestic, industrial, energy and livestock use. Unconsumed irrigation water is returned to the**
147 **soil column of the hydrological model. Unconsumed water for the other sectors is returned to the river streamflow.**
148 **Small reservoirs fill using surface runoff from the cell they are located, while large dam reservoirs operate solely on**
149 **river streamflow.**

150 **2.2.1 Water withdrawal and consumption**

151 In VIC-WUR, sectoral water demands need to be specified for each grid cell (Section 2.3). To meet
152 water demands, water can be withdrawn from river streamflow, small (within-grid) reservoirs, and
153 groundwater resources. Streamflow withdrawals are abstracted from the grid cell discharge (as
154 generated by the routing module) and reservoir withdrawals are abstracted from small dam reservoirs
155 (located in the cell). Groundwater withdrawals are abstracted from the third layer soil moisture and an
156 (unlimited) aquifer below the soil column. Aquifer abstractions represent renewable and non-renewable
157 abstractions from deep groundwater resources. Subsurface runoff is used to fill the aquifer if there is a
158 deficit.

159 The partitioning of water withdrawals between surface and ground water resources is data driven
160 (similar to e.g. Döll et al., 2012; Voisin et al., 2017; Hanasaki et al., 2018). Partitioning was based on
161 the study of Döll et al. (2012), who estimated groundwater withdrawal fractions for each sector in around
162 15.000 national and sub-national administrative units. These groundwater fractions were based mainly
163 on information from the International Groundwater Resources Assessment Centre (IGRAC; un-
164 igrac.org) database. Surface water withdrawals were partitioned between river streamflow and small
165 reservoirs relative to water availability. Groundwater withdrawals were first withdrawn from the third
166 soil layer, second from the (remaining) river streamflow resources and lastly from the groundwater
167 aquifer. This order was implemented to avoid overestimation of non-renewable groundwater
168 withdrawals as a result of errors in the partitioning data. Aquifer withdrawals are additionally limited
169 by the pumping capacity from Sutanudjaja et al. (2018), who estimated regional pumping capacities
170 based on information from IGRAC.

171 Water can also be withdrawn from the river streamflow of other ‘remote’ cells in delta areas. Since
172 rivers cannot split in the routing module, the model is unable to simulate the redistribution of water
173 resources in dendritic deltas. Therefore, streamflow at the river mouth is available for use in delta areas
174 (partitioned based on demand) to simulate the actual water availability. Delta areas were delineated by
175 the global delta map of Tessler et al. (2015).

176 In terms of water allocation, under conditions where water demands cannot be met, water withdrawals
177 are allocated to the domestic, energy, manufacturing, livestock and irrigation sector in that order.
178 Withdrawn water is partly consumed, meaning the water evaporates and does not return to the
179 hydrological model. Consumption rates were set at 0.15 for the domestic and 0.10 for the industrial
180 sector, based on the data of Shiklomanov (2000). The water consumption in the energy sector was based
181 on Goldstein and Smith (2002) and varies per thermoelectric plant based on the fuel type and cooling
182 system. For the livestock sector the assumption was made that all withdrawn water is consumed.
183 Unconsumed water withdrawals for these sectors are returned as river streamflow. For the irrigation
184 sector, consumption was determined by the calculated evapotranspiration. Unconsumed irrigation water
185 remains in the soil column and eventually returns as subsurface runoff.

186 2.2.2 Environmental flow requirements

187 Water withdrawals can be constrained by environmental flow requirements (EFRs). These EFRs specify
188 the timing and quantity of water needed to support terrestrial river ecosystems (Smakhtin et al., 2004;
189 Pastor et al., 2019). Surface and groundwater withdrawals are constrained separately in VIC-WUR,
190 based on the EFRs for streamflow and baseflow respectively. EFRs for streamflow specify the minimum
191 river streamflow requirements while EFRs for baseflow specify the minimum subsurface runoff
192 requirements (from groundwater to surface water). Since baseflow is a function groundwater
193 availability, baseflow requirements are used to constrain groundwater (including aquifer) withdrawals.

194 Various EFR methods are available (Smakhtin et al., 2004; Richter et al., 2012; Pastor et al., 2014). Our
195 study used the Variable Monthly Flow (VMF) method (Pastor et al., 2014) to calculate the EFRs for
196 streamflows. VMF calculates the required streamflow as a fraction of the natural flow during high (30
197 %), intermediate (45 %) and low (60 %) flow periods, as described in Appendix B. The VMF method
198 performed favourably compared to other hydrological methods, in 11 case studies where EFRs were
199 calculated locally (Pastor et al., 2014). The advantage of the VMF method is that the method accounts
200 for the natural flow variability, which is essential to support freshwater ecosystems (Poff et al., 2010).

201 EFR methods for baseflow have been rather underdeveloped compared to EFR methods for streamflow.
202 However, a presumptive standard of 90 % of the natural subsurface runoff through time was proposed
203 by Gleeson and Richter (2018), as described in Appendix B. This standard should provide high levels
204 of ecological protection, especially for groundwater dependent ecosystems.

205 Note that part of the EFRs for baseflow are already captured in the EFRs for streamflow, especially
206 during low-flow periods that are usually dominated by baseflows. However, the EFRs for baseflow
207 specifically limit local groundwater withdrawals while EFRs for streamflow include the accumulated
208 runoff from upstream areas. Also, the chemical composition of groundwater derived flows is inherently
209 different, making them a non-substitutable water flow for environmental purposes (Gleeson and Richter,
210 2018).

211 **2.2.3 Dam operation**

212 Due to the lack of globally available information on local dam operations, several generic dam operation
213 schemes were developed for macro-scale hydrological models to reproduce the effect of dams on natural
214 streamflow (Haddeland et al., 2006a; Hanasaki et al., 2006; Zhao et al., 2016; Rougé et al., 2019; Yassin
215 et al., 2019). In VIC-WUR a distinction is made between ‘small’ dam reservoirs (with an upstream area
216 smaller than the cell area) and ‘large’ dam reservoirs, similar to Hanasaki et al. (2018), Wisser et al.
217 (2010a) and Döll et al. (2009). Small dam reservoirs act as buckets that fill using surface runoff of the
218 grid-cell they are located in and reservoirs storage can be used for water withdrawals in the same cell.
219 Large dam reservoirs are located in the main river and used the operation scheme of Hanasaki et al.
220 (2006), as described in Appendix C.

221 The scheme distinguishes between two dam types: (1) dams that do not account for water demands
222 downstream (e.g. hydropower dams or flood protection dams) and (2) dams that do account for water
223 demand downstream (e.g. irrigation dams). For dams that do not account for demands, dam release is
224 aimed at reducing annual fluctuations in discharge. For dams that do account for demands, dam release
225 is additionally adjusted to provide more water during periods of high demand. The operation scheme
226 was validated by Hanasaki et al. (2006) for 28 reservoirs and was used in various other studies (Hanasaki
227 et al., 2008a; Döll et al., 2009; Pokhrel et al., 2012b; Voisin et al., 2013; Hanasaki et al., 2018). Here,
228 the scheme was adjusted slightly to account for monthly varying EFRs and to reduce overflow releases,
229 which is described in Appendix C.

230 The Global Reservoir and Dam (GRanD) database (Lehner et al., 2011) was used to specify location,
231 capacity, function (purpose), and construction year of each dam. The capacity of multiple (small- and
232 large) dams located in the same cell were combined.

233 **2.3 Sectoral water demands**

234 VIC-WUR water withdrawals are based on the irrigation, domestic, industry, energy and livestock water
235 demand in each grid-cell. Water demands represent the potential water withdrawal, which is reduced
236 when insufficient water is available. Irrigation demands were estimated based on the hydrological model

237 while water demands for other sectors are provided to the model as an input. Domestic and industrial
238 were estimated based on several socioeconomic predictors, while energy and livestock water demands
239 were derived from power plant and livestock distribution data. Due to data limitations the energy sector
240 was incomplete, and energy water demands were partly included in the industrial water demands (which
241 combined the remaining energy and manufacturing water demands). For more details concerning
242 sectoral water demand calculations the reader is referred to Appendix D.

243 **2.3.1 Irrigation demands**

244 Irrigation demands were set to increase soil moisture in the root zone so that water availability is not
245 limiting crop evapotranspiration and growth. The exception is paddy rice irrigation (Brouwer et al.,
246 1989), where irrigation was also supplied to keep the upper soil layer saturated. Water demands for
247 paddy irrigation practices are relatively high compared to conventional irrigation practices due to
248 increased evaporation and percolation. Therefore, the crop irrigation demands for these two irrigation
249 practices were calculated and applied separately (i.e. in different sub-grids). Note that multiple cropping
250 seasons are included based on the MIRCA2000 land-use dataset (Portmann et al., 2010) (see Section
251 3.1 for more details).

252 Total irrigation demands also included transportation and application losses. Note that transportation
253 and application losses are not 'lost' but rather returned to the soil column without being used by the
254 crop. The water loss fraction was based on Frenken and Gillet (2012), who estimated the irrigation
255 efficiency for 22 United Nations sub-regions. Irrigation efficiencies were estimated based on the
256 differences between the calculated crop water requirements (crop evapotranspiration; consumptive
257 water use) and the reported irrigation water withdrawals (including transportation and application
258 losses). Crop water requirements are estimated based on the FAO Irrigation and Drainage paper (Allen
259 et al., 1998). Low irrigation efficiencies can result in irrigation water withdrawals up to four times higher
260 than the crop water requirements in regions such as east- and west Africa.

261 **2.3.2 Domestic and industrial demands**

262 Domestic and industrial water withdrawals were estimated based on Gross Domestic Product (GDP) per
263 capita and Gross Value Added (GVA) by industries respectively (from Bolt et al. (2018), Feenstra et al.
264 (2015) and World bank (2010); see Appendix D for more details). These drivers do not fully capture the
265 multitude of socioeconomic factors that influence water demands (Babel et al., 2007). However, the
266 wide availability of data allows for extrapolation of water demands to data-scarce regions and future
267 scenarios (using studies such as Chateau et al. (2014)).

268 Domestic water demands per capita (used for drinking, sanitation, hygiene and amenity uses) were
269 estimated similar to Alcamo et al. (2003). Demands increased non-linearly with GDP per capita due to
270 the acquisition of water using appliances as household become richer. A minimum water supply is
271 needed for survival, and the saturation of water using appliances sets a maximum on domestic water
272 demands. Industrial water demands (used for cooling, transportation and manufacturing) were estimated
273 similar to Flörke et al. (2013) and Voß and Flörke (2010). Industrial demands increased linearly with
274 GVA (as an indicator of industrial production). Since industrial water intensities (i.e. the water use per
275 production unit) vary widely between different industries (Flörke and Alcamo, 2004 ; Vassolo and Döll,
276 2005; Voß and Flörke, 2010), the average water intensity was estimated for each country. Both domestic
277 and industrial water demands were also influenced by technological developments that increase water-
278 use efficiency over time, as in Flörke et al. (2013).

279 Domestic water demands varied monthly based on air temperature variability as in Huang et al. (2018)
280 (based on Wada et al. (2011b)). Using this approach, water demands were higher in summer than in
281 winter, especially for counties with strong seasonal temperature differences. Domestic water demand
282 per capita were downscaled using the HYDE3.2 gridded population maps (Goldewijk et al., 2017).
283 Industrial water demands were kept constant throughout the year. Industrial demands were downscaled
284 from national to grid cell values using the NASA Back Marble night-time light intensity map (Roman
285 et al., 2018). National industrial water demands were allocated based on the relative light intensity per
286 grid cell for each country.

287 **2.3.3 Energy and livestock demands**

288 Energy water demands (used for cooling of thermoelectric plants) were estimated using data from van
289 Vliet et al. (2016). Water use intensity for generation (i.e. the water use per generation unit) was
290 estimated based on the fuel and cooling system type (Goldstein and Smith, 2002), which was combined
291 with the generation capacity. Note that the data only covered a selection of the total number of
292 thermoelectric power plants worldwide. Around 27 % of the total (non-renewable) global installed
293 capacity between 1980 and 2011 was included in the dataset due to lack of information on cooling
294 system types for the majority of thermoelectric plants. To avoid double counting, energy water demands
295 were subtracted from the industrial water demands.

296 Livestock water demands (used for drinking and animal servicing) were estimated by combining the
297 Gridded Livestock of the World (GLW3) map (Gilbert et al., 2018) with the livestock water requirement
298 reported by Steinfeld et al. (2006). Eight varieties of livestock were considered: cattle, buffaloes, horses,
299 sheep, goats, pigs, chicken and ducks. Drinking water demands varied monthly based on temperature as
300 described by Steinfeld et al. (2006), whereby drinking water requirements were higher during higher
301 temperatures.

302 **3 Model application**

303 **3.1 Setup**

304 VIC-WUR results were generated between 1979 and 2016, excluding a spin-up period of one year
305 (analysis period from 1980 to 2016). The model used a daily timestep (with a 6-hourly timestep for snow
306 processes) and simulations were executed on a 0.5° by 0.5° grid (around 55 km at the equator) with three
307 soil layers per grid cell. Soil and (natural) vegetation parameters were the same as in Nijssen et al.
308 (2001c) (disaggregated to 0.5°), who used various sources to determine the soil (Cosby et al., 1984;
309 Carter and Scholes, 1999) and vegetation parameters (Calder, 1993; Ducoudre et al., 1993; Sellers et al.,
310 1994; Myneni et al., 1997).

311 Nijssen et al. (2001c) used the Advanced Very High Resolution Radiometer vegetation type database
312 (Hansen et al., 2000) to spatially distinguish 13 land cover types. The land cover type ‘cropland’ in the

313 original land-cover dataset was replaced by cropland extents from the MIRCA2000 cropland dataset
314 (Portmann et al., 2010). MIRCA2000 distinguishes the monthly growing area(s) and season(s) of 26
315 irrigated and rain-fed crop types around the year 2000. Crop types were aggregated into three land cover
316 types: rain-fed, irrigated and paddy rice cropland. The natural vegetation was proportionally rescaled to
317 make up discrepancies between the natural vegetation and cropland extents.

318 Cropland coverage (the cropland area actually growing crops) varied monthly based on the crop growing
319 areas of MIRCA2000. The remainder was treated as bare soil. Cropland vegetation parameters (e.g. Leaf
320 Area Index (LAI), displacement, vegetation roughness and albedo) vary monthly based on the crop
321 growing seasons and the development-stage crop coefficients of the Food and Agricultural Organisation
322 (Allen et al., 1998).

323 The latest WATCH forcing data Era Interim (aggregated to 6 hourly), developed by the EU Water and
324 Global Change (WATCH; Harding et al., 2011) project, was used as climate forcing (WFDEI; Weedon
325 et al., 2014). The dataset provides gridded historical climatic variables of minimum and maximum air
326 temperature, precipitation (as the sum of snowfall and rainfall, GPCC bias-corrected), relative humidity,
327 pressure and incoming shortwave and longwave radiation.

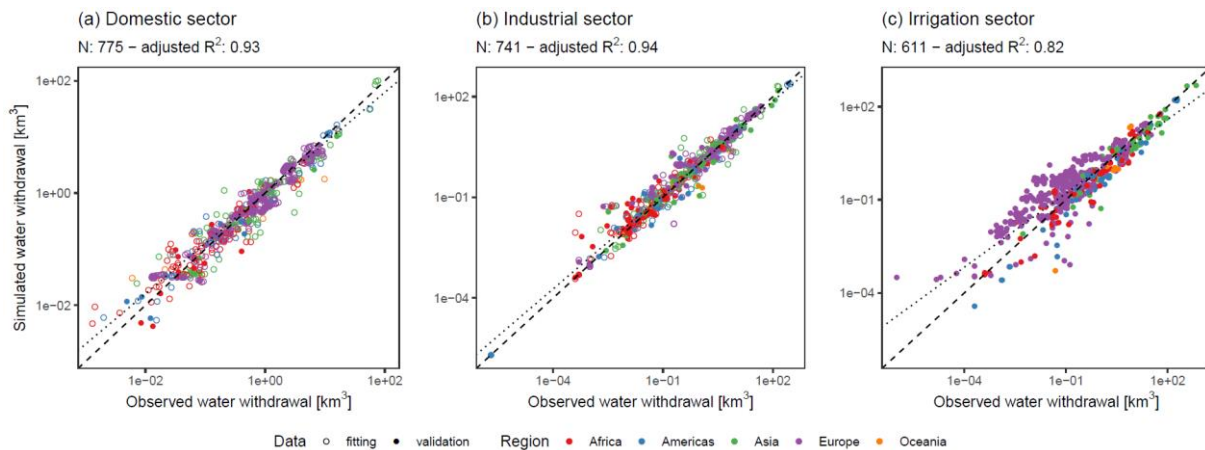
328 For naturalized simulations only the routing module was used. For the human-impact simulations the
329 sectoral water withdrawals and dam operation modules were turned on in the model simulations. For
330 the EFR-limited simulations water withdrawals and dam operations were constrained as described.

331 **3.2 Validation and evaluation**

332 In order to validate the VIC-WUR human-impact modules, water withdrawal, terrestrial total water
333 storage anomalies, streamflow and reservoir operation simulations were compared with observations.
334 The validation specifically focused on the effects of the newly included human-impact modules,
335 meaning that streamflow and total-water storage anomaly results are shown for river basins that are
336 strongly influenced by human activities. A general validation for streamflow and terrestrial total water
337 storage anomalies (including basins with limited human activities) is shown in Appendix E.

338 3.2.1 Sectoral water withdrawals

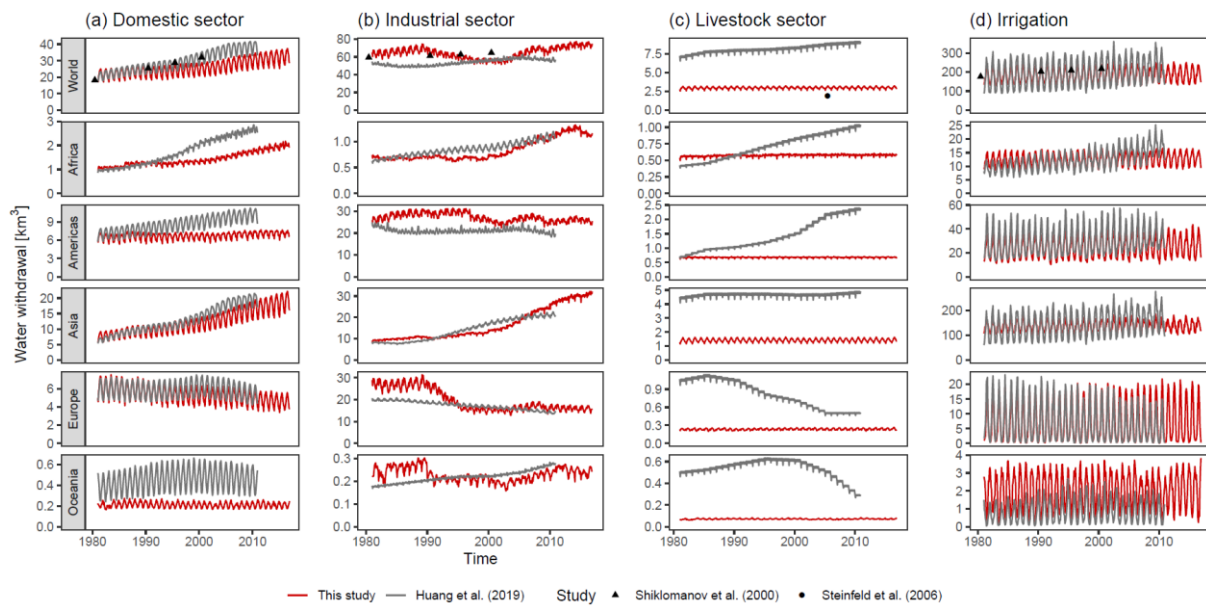
339 Simulated global domestic, industrial, livestock and irrigation mean water withdrawals were 310, 771,
340 36 and 2202 km³ year⁻¹ respectively for the period of 1980 to 2016. Sectoral water withdrawals were
341 compared with FAO national annual water withdrawals (FAO, 2016), monthly withdrawal data from
342 Huang et al. (2018) and annual withdrawal data from Shiklomanov (2000) and Steinfeld et al. (2006).
343 For the latter studies, water withdrawals were aggregated by region (world, Africa, Asia, Americas,
344 Europe and Oceania). Note that Huang et al. (2018) irrigation water withdrawals integrate results of four
345 other macro-scale hydrological models (WaterGAP, H08, LPJmL, PCR-GLOBWB), using the same
346 land-use and climate setup as our study. Results from individual macro-scale hydrological models are
347 also shown.



349 **Figure 2: Comparison between simulated and reported national annual water withdrawals for the (a) domestic, (b)**
350 **industrial and (c) irrigation sector. Colours distinguish between regions. Open circles were also used in the calibration**
351 **of the water withdrawal demands. The dashed line indicates the 1:1 ratio and the spotted line indicates the simulated**
352 **best linear fit. Note the log-log axis which is used to display the wide range of water withdrawals. The R² adjusted is**
353 **also based on the log values.**

354 Simulated domestic, industrial and irrigation water withdrawals correlated well to reported national
355 water withdrawals, with adjusted R² of 0.93, 0.94 and 0.82 for domestic, industrial and irrigation water
356 withdrawal respectively (Figure 2a-c). Generally, smaller water withdrawals were overestimated and
357 larger water withdrawals were underestimated. Differences for the domestic and industrial sector were
358 small and probably related to the fact that smaller countries were poorly delineated on a 0.5° by 0.5°
359 grid. However, irrigation differences were larger with overestimations of irrigation water withdrawals
360 in (mostly) Europe. Since irrigation water demands are the results of the simulated water balance,

361 overestimations would indicate a regional underestimation of water availability for Europe or
 362 differences in irrigation efficiency.



363
 364 **Figure 3: Comparison between simulated and compiled monthly and annual regional water withdrawals for the (a)**
 365 **domestic sector, (b) industrial sector and (c) irrigation. Colours and shapes distinguish between studies. Note that the**
 366 **jitter in livestock withdrawals is due to the different days per month.**

367 When domestic, industrial and livestock water withdrawals were compared to other studies, results were
 368 mixed (figure 3a-c). Simulated domestic withdrawals followed a similar trend in time. However,
 369 simulated domestic water withdrawals trends were overall somewhat underestimated with a mean bias
 370 of 54 km³ year⁻¹ compared to Huang et al. (2018). Asia is the main contributor to the global
 371 underestimation, but results are similar in most regions. Simulated industrial water withdrawal were
 372 (mostly) higher in our study with a mean bias of 107 km³ year⁻¹ compared to Huang et al. (2018) but
 373 only a mean bias of 5 km³ year⁻¹ compared to Shiklomanov (2000). Also, industrial water withdrawal
 374 trends in time were less consistent.

375 Withdrawal differences for the domestic and industrial sector are probably due to the limited data
 376 availability. Our approach to compute water demands was data-driven and sensitive to data gaps (as
 377 opposed to Huang et al. (2018) who also combined model results). For example, domestic withdrawal
 378 data for China was not available before 2007 and industrial withdrawal data was limited before 1990.

379 For livestock water withdrawals there is a large discrepancy between the Huang et al. (2018) and
 380 Steinfeld et al. (2006). Both studies used similar livestock maps, but there was large differences in
 381 livestock water intensity [litre animal⁻¹ year⁻¹]. Since our study used Steinfeld et al. (2006) to estimate
 382 livestock water intensity, our results were closer to their values (slightly higher due to the inclusion of
 383 buffaloes, horses and ducks). Note that Huang et al. (2018) shows trends in livestock water withdrawals
 384 while our study used static livestock maps.

385 **Table 1: Global irrigation water withdrawals as calculated by several global hydrological models. **Includes livestock**
 386 **withdrawals.**

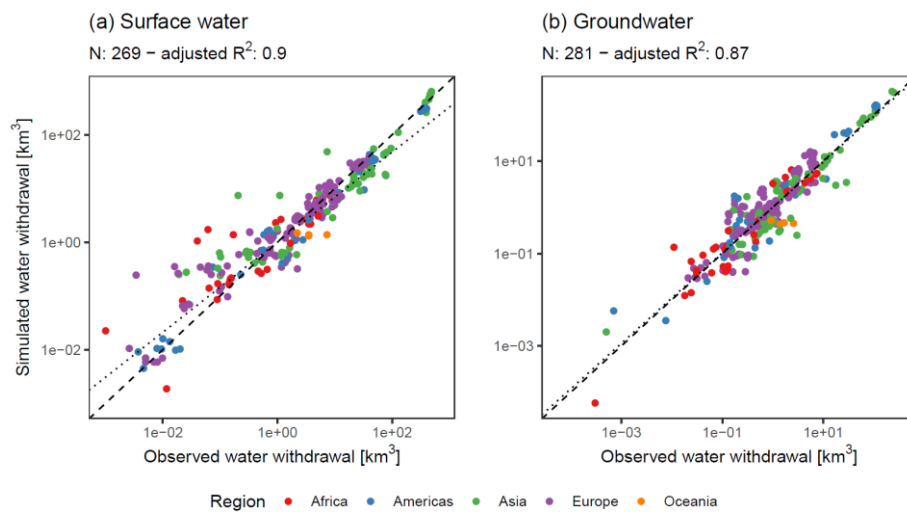
Model	Irrigation withdrawal [km ³ year ⁻¹]	Representative years	Reference
VIC-WUR	2202 (± 60)	1980-2016	Our study
H08	(a) 2810 (b) 2544 (± 75)	(a) 1995 (b) 1984 - 2013	(a) Hanasaki et al. (2008b) (b) Hanasaki et al. (2018)
MATSIRO	(a) 2158 (± 134) (b) 3028 (± 171)	(a) 1983 - 2007 (b) 1998 - 2002	(a) Pokhrel et al. (2012a) (b) Pokhrel et al. (2015)
LPJmL	2555	1971 - 2000	Rost et al. (2008)
PCR-GLOB	(a) 2644 (b) 2309 **	(a) 2010 (b) 2000 - 2015	(a) Wada and Bierkens (2014) (b) Sutanudjaja et al. (2018)
WaterGAP	(a) 3185 (b) 2400	(a) 1998-2002 (b) 2003 - 2009	(a) Döll et al. (2012) (b) Döll et al. (2014)
WBM	2997	2002	Wisser et al. (2010b)

387 Simulated irrigation water withdrawals were within range of other macro-scale hydrological model
 388 estimates (Table 1). Simulated monthly variability in irrigation water withdrawals is reduced compared
 389 to the compiled results of Huang et al. (2018) (Figure 3d), especially in Asia. Also, trends in time are
 390 less pronounced as can be seen in Africa. These differences may indicate a relative low weather/climate
 391 sensitivity of evapotranspiration in VIC-WUR, as annual and interannual weather changes affect
 392 irrigation water demands to a lesser degree.

393 **3.2.2 Groundwater withdrawals and depletion**

394 Simulated global mean withdrawals were 2327 and 992 km³ year⁻¹ for surface and groundwater
 395 respectively for the period of 1980 to 2016. Of the global groundwater withdrawals, 334 km³ year⁻¹

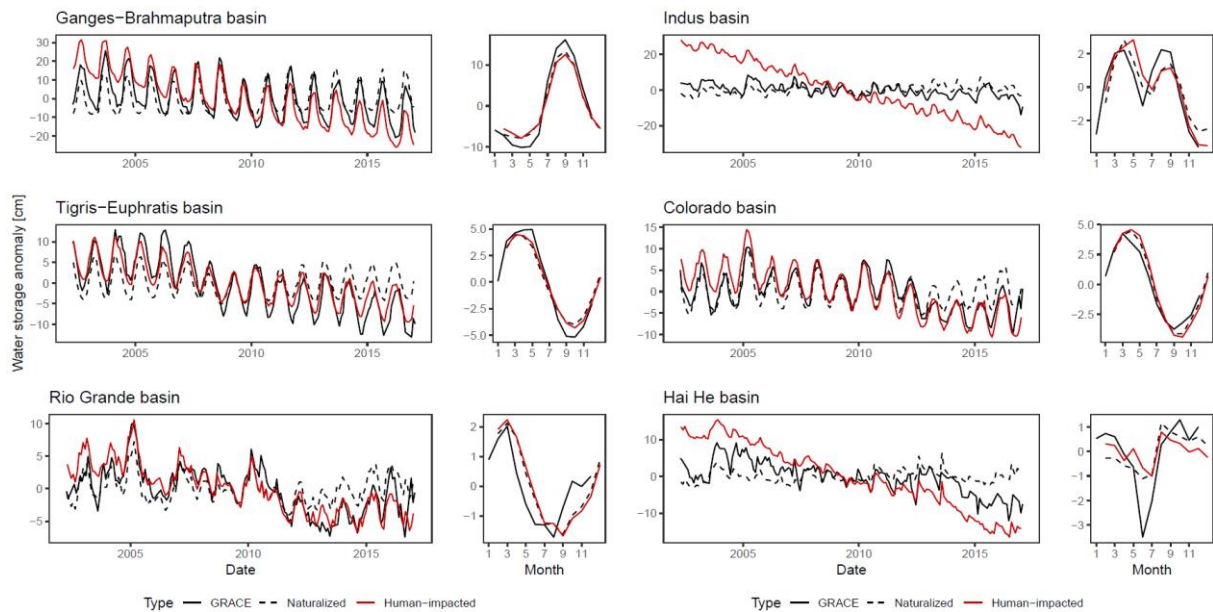
396 contributed to groundwater depletion. Simulated ground and surface water withdrawals and terrestrial
 397 total water storage anomalies were compared FAO national annual water withdrawals (FAO, 2016) and
 398 monthly storage anomaly data from the GRACE satellite (NASA, 2002). GRACE satellite total water
 399 storage anomalies were used to validate total water storage dynamics as well as groundwater exploitation
 400 contributing to downward trends in total water storage. Groundwater depletion results from other macro-
 401 scale hydrological models are shown as well. In order to compare the simulation results to the GRACE
 402 dataset, a 300km gaussian filter was applied to the simulated data (similar to Long et al. (2015)).



403

404 **Figure 4: Comparison between simulated and reported national annual water withdrawals from (a) surface water and**
 405 **(b) groundwater. Colours distinguish between regions. The dashed line indicates the 1:1 ratio and the spotted line**
 406 **indicates the simulated best linear fit. Note the log-log axis which is used to display the wide range of water withdrawals.**
 407 **The R² adjusted is also based on the log values.**

408 Simulated surface and groundwater withdrawals correlated well to the reported national water
 409 withdrawals, with adjusted R² of 0.90 and 0.87 for surface and groundwater respectively (Figure 4a-b).
 410 Surface water withdrawals were overestimated for low withdrawals and underestimated for large
 411 withdrawals. There is a weak correlation (-0.35) between the underestimations in surface water
 412 withdrawals and the overestimation in groundwater withdrawals, meaning water withdrawal differences
 413 could be related to the partitioning between surface and groundwater resources. Also, it is likely that
 414 low water demands are overestimated (as discussed in Section 3.2.1), resulting in an overestimation of
 415 low surface water withdrawals.



416

417 **Figure 5: Comparison between simulated and observed monthly terrestrial total water storage anomalies. Figures**
 418 **indicate timeseries and multi-year mean average for naturalized simulations (dashed), human-impacted simulations**
 419 **(red) and observed (black) terrestrial total water storage anomalies.**

420 Simulated monthly terrestrial water storage anomalies correlated well to the GRACE observations, with
 421 mean annual and inter-annual Root Mean Squared Error (RMSE) of 1.9 mm and 3.5 mm respectively.
 422 The difference between annual and inter-annual performance was primarily due to the groundwater
 423 depletion process (Figure 5). Simulated groundwater depletion was (mostly) overestimated (e.g. Indus
 424 and Hai He basins), with higher declining trends in terrestrial total water storage for most basins.
 425 However, compared to other macro-scale hydrological models, simulated groundwater withdrawal and
 426 exploitation was within range (Table 2), even though total groundwater withdrawals were relatively
 427 high.

428 As with the FAO comparison, these results seems to indicate that withdrawal partitioning towards
 429 groundwater is overestimated. However, conclusions regarding groundwater depletion are limited by
 430 the relatively simplistic approach to groundwater used in our study (as discussed by Konikow (2011)
 431 and de Graaf et al. (2017)). For example, processes such as wetland recharge and groundwater flows
 432 between cells are not simulated, even though these could decrease groundwater depletion.

433 **Table 2: Global groundwater withdrawals and depletion as calculated by several global hydrological models.**

Model	Groundwater withdrawal [km ³ year ⁻¹]	Groundwater depletion [km ³ year ⁻¹]	Representative years	Reference
-------	--	---	----------------------	-----------

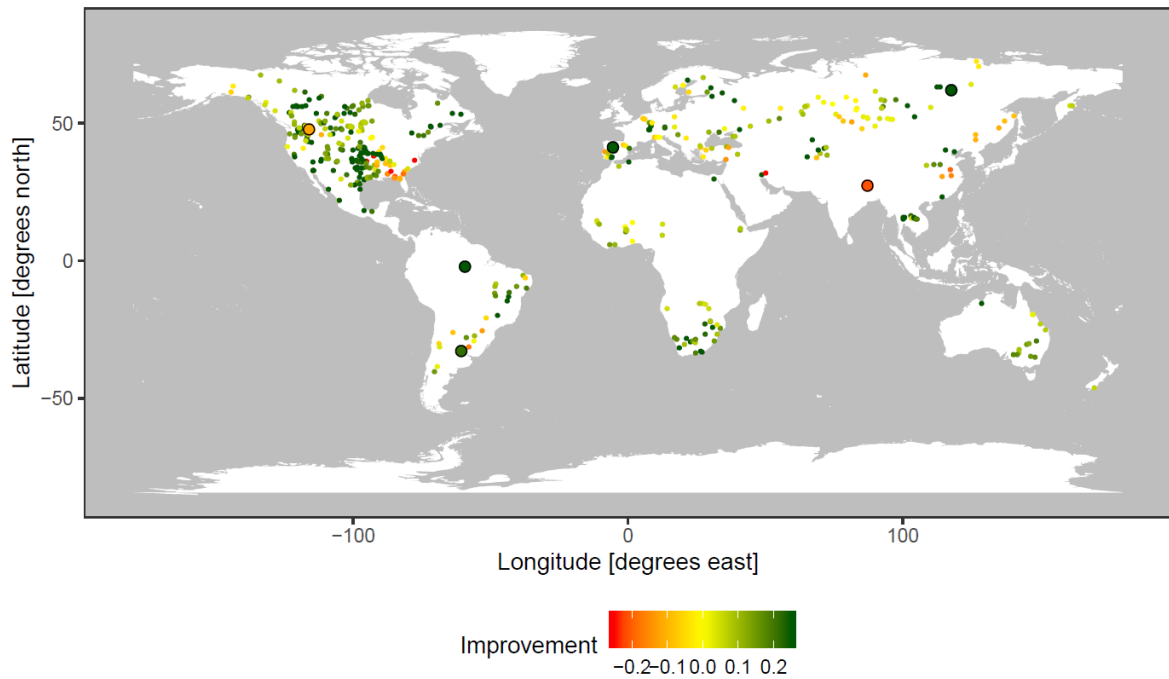
VIC-WUR	992 (\pm 51)	316 (\pm 63)	1980 - 2016	Our study
H08	789 (\pm 30)	182 (\pm 26)	1984 - 2013	Hanasaki et al. (2018)
MATSIRO	570 (\pm 61)	330	1998 - 2002	Pokhrel et al. (2015)
GCAM		(a) 600 (b) 550	(a) 2005 (b) 2000	(a) Kim et al. (2016) (b) Turner et al. (2019)
PCR-GLOB	(a) 952 (b) 632	(a) 304 (b) 171	(a) 2010 (b) 2000 - 2015	(a) Wada and Bierkens (2014) (b) Sutanudjaja et al. (2018)
WaterGAP	(a) 1519 (b) 888	(a) 250 (b) 113	(a) 1998-2002 (b) 2000 - 2009	(a) Döll et al. (2012) (b) Döll et al. (2014)

434 3.2.3 Discharge modification

435 Simulated discharge was compared to GRDC station data (GRDC, 2003) for various human-impacted
436 rivers. Stations were selected if the upstream area was larger than 20,000 km², matched the simulated
437 upstream area at the station location, and the available data spanned more than 2 years. Subsequently,
438 stations where the human-impact modules did not sufficiently impacted discharge were omitted. In order
439 validate the reservoir operation more thoroughly, simulated reservoir inflow, storage and release was
440 compared with operation data from Hanasaki et al. (2006) and Yassin et al. (2019). Reservoirs were
441 included if the simulated storage capacity (which is the combined storage capacity of all large dams in
442 a grid) was similar to observed storage capacity.

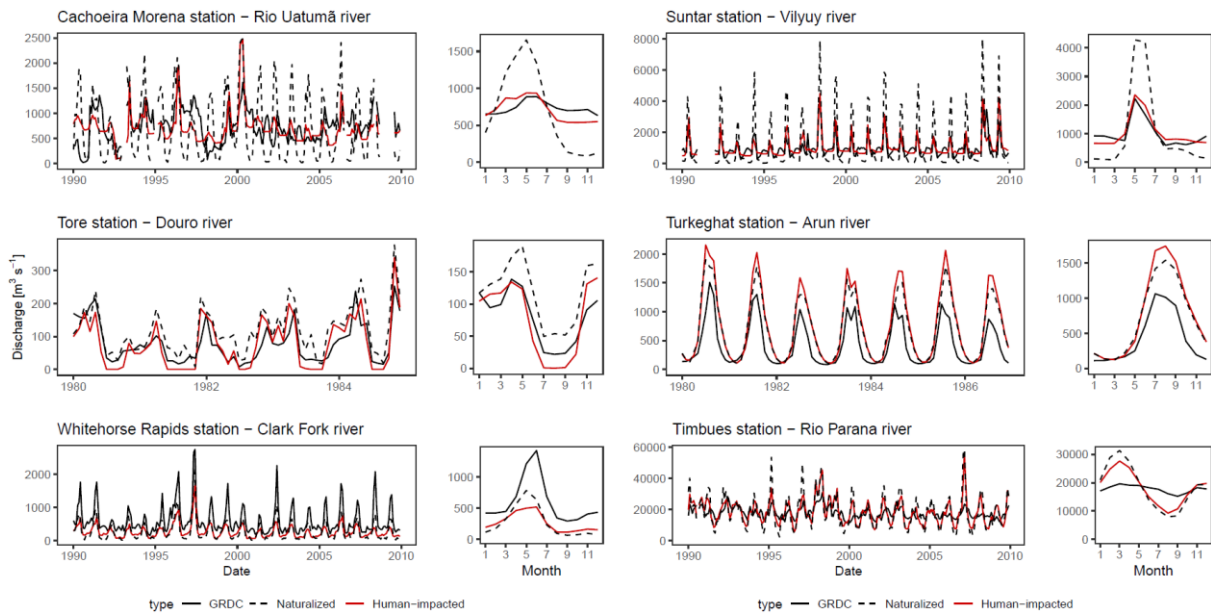
Discharge improvement

N: 462 – improved: 370



443

444 **Figure 6: Discharge improvement from naturalized to human-impacted simulations (as a fraction of the naturalized**
 445 **RMSE). Circled larger stations are shown in Figure 7.**



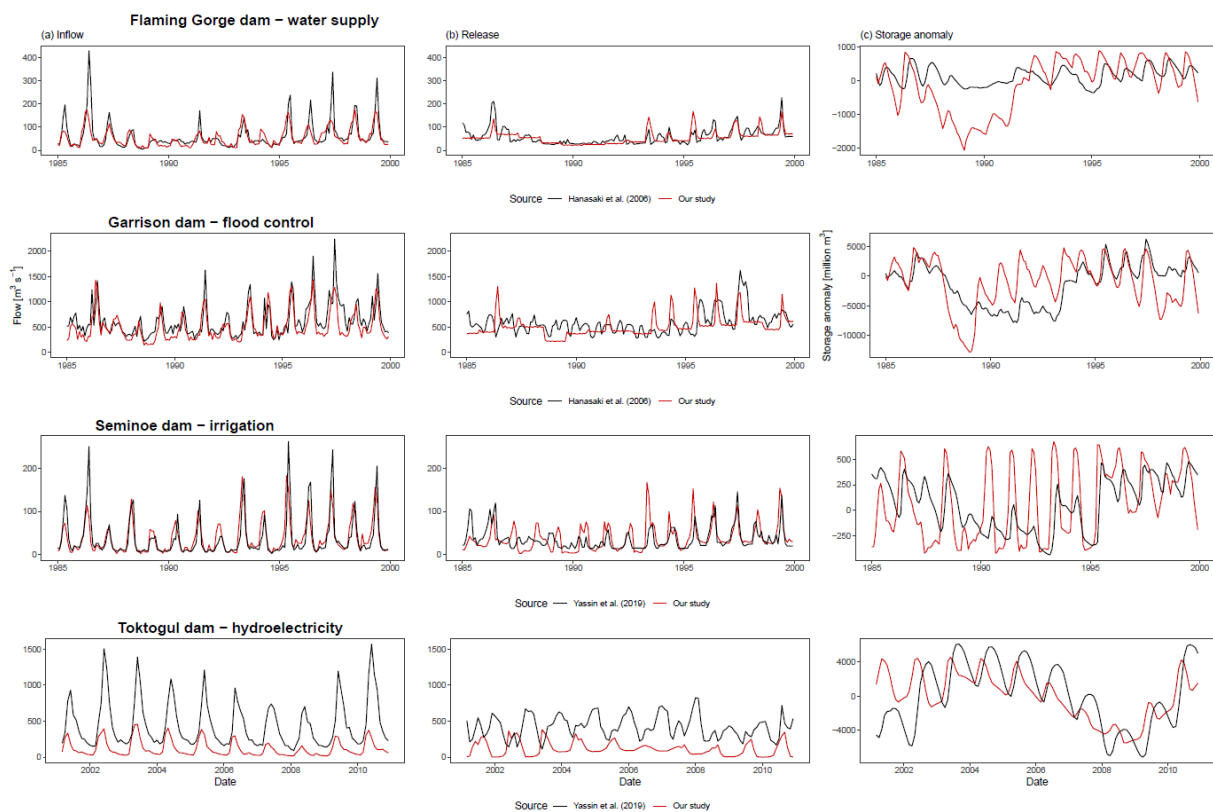
446

447 **Figure 7: Comparison between simulated and observed discharge. Figures indicate timeseries and multi-year average**
 448 **of for naturalized simulations (dashed), human-impacted simulations (red) and observed (black) discharge.**

449 The inclusion of the human-impact modules improved discharge performance, measured in RMSE, for
 450 370 out of 462 stations (80 %; Figure 6 and 7). Improvements were mainly due to the effects of reservoir
 451 operation on discharges (e.g. Cachoeira Morena and Suntar stations), but also due to withdrawal

452 reductions (e.g. Tore station). Reservoir effects on discharge were sometimes underestimated however
 453 (e.g. Timbues station).

454 Decreased performance was mostly related to under or overestimations of (calibrated) natural
 455 streamflow which was subsequently exacerbated by reservoir operation and water withdrawals. For
 456 example, the Clark Fork river naturalized streamflow was underestimated, which was subsequently
 457 further underestimated by the human-impact modules (Whitehorse Rapids station). Also, increases in
 458 discharge due to groundwater withdrawals could increase naturalized streamflow (e.g. Turkeghat
 459 station). Further improvements to discharge performance would most likely require either a recalibration
 460 of the VIC model parameters.



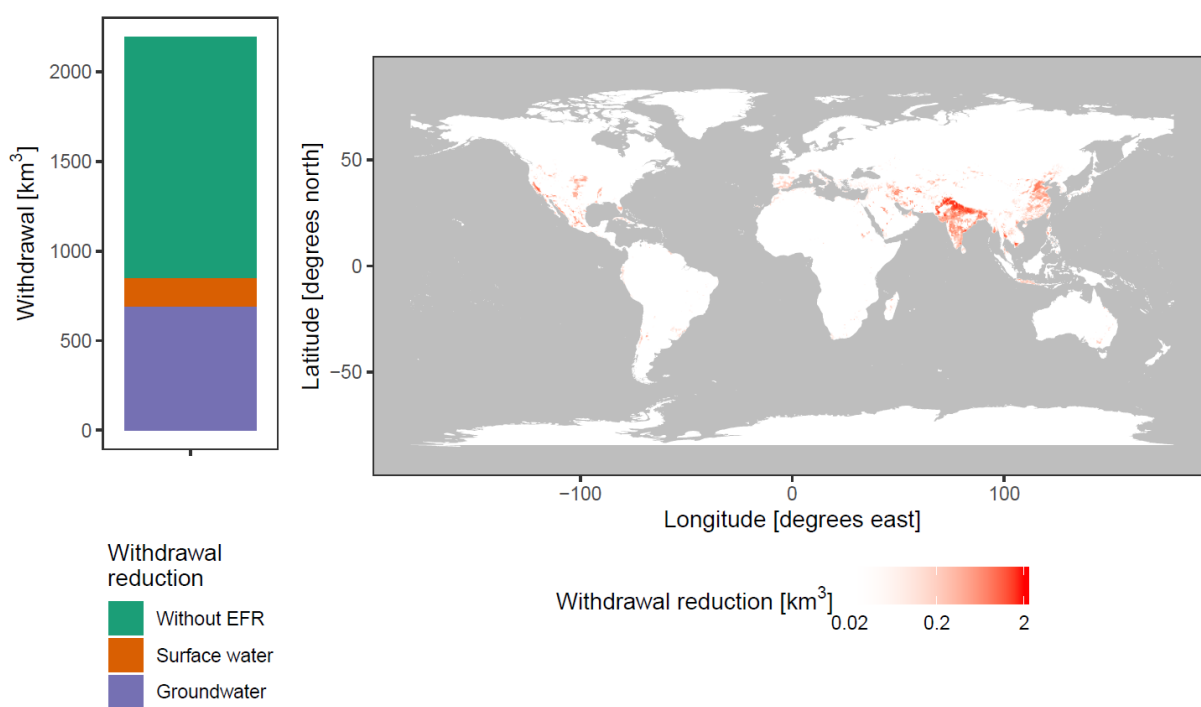
461
 462 **Figure 8: Comparison between simulated and observed reservoir operation. Figures indicate timeseries and multi-year**
 463 **averages of (a) inflow, (b) release and (c) storage anomalies for human-impacted simulations (red) and observations**
 464 **(black).**

465 For individual reservoirs, operation characteristics were generally well simulated (Figure 8), with
 466 reductions in annual discharge variations (e.g. Flaming Gorge and Garrison dams) and increased water
 467 release for irrigation (e.g. Seminoe dam). However, due to changes in locally simulated and actual
 468 inflow, dam operation can take on different characteristics (e.g. Toktogul dam). Also, peak discharge

469 events caused by reservoir overflow (as also described by Masaki et al. (2018a)) were not always
 470 sufficiently represented in the observations (e.g. Garisson dam). These differences indicate locally
 471 varying reservoir operation strategies. Several studies have developed reservoir operation schemes that
 472 can be calibrated to the local situation (Rougé et al., 2019; Yassin et al., 2019). However, worldwide
 473 implementations of these operation schemes remains limited by data availability.

474 3.3 Integrated environmental flow requirements

475 In order to assess the impact and capabilities of the newly integrated environmental flow requirements
 476 (EFRs) module, simulated water withdrawals with and without adhering to EFRs were compared.



478 **Figure 9: Average annual irrigation water withdrawal reductions when adhering to EFRs as (left) global gross total and**
 479 **(right) spatially distributed. Global gross totals are separated into withdrawals without any reduction (green), surface**
 480 **water withdrawal reductions (orange) and groundwater withdrawal reductions (purple). Note the log axis for the**
 481 **spatially distributed withdrawal reductions to better display the spatial distribution of the reductions.**

482 If water-use would be limited to EFRs, irrigation withdrawals would need to be reduced by about 39 %
 483 ($851 \text{ km}^3 \text{ year}^{-1}$) (Figure 9a). Under the strict requirements used in our study, 81 % ($693 \text{ km}^3 \text{ year}^{-1}$) of
 484 the reduction could be attributed to limitations imposed on groundwater withdrawals. Subsequently, the
 485 impact of the environmental flow requirements (if adhered to) would be largest in groundwater
 486 dependent regions (Figure 9b). Note that, due to the full integration of EFRs, downstream surface water

487 withdrawals increased by $98 \text{ km}^3 \text{ year}^{-1}$ when limiting groundwater withdrawals on top of limiting
488 surface water withdrawals, due to increase subsurface runoff.

489 Reductions due to EFRs were similar to Jägermeyr et al. (2017), who calculated irrigation withdrawal
490 reductions of 41 % ($997 \text{ km}^3 \text{ year}^{-1}$) assuming only surface water abstractions. In our study, surface
491 water reductions were smaller since the strict groundwater requirements increases subsurface runoff to
492 surface waters. It can be discussed to what extent the EFRs for baseflow were too constricting, since
493 they were based on the relatively stringent EFR for streamflow of Richter et al. (2012) (10 % of the
494 natural streamflow). However, in the absence of any other standards, this baseflow standard remains the
495 best available. Note that, even when accounting for EFRs for baseflow on a grid scale, withdrawals
496 could still have local and long-term impacts that are not captured by the model. The timing, location and
497 depth of groundwater withdrawals are important factors due to their interactions with the local
498 geohydrology, as discussed by Gleeson and Richter (2018).

499 **4 Conclusion**

500 The VIC-WUR model introduced in this paper aims to provide new opportunities for global water
501 resource assessments using the VIC model. Accordingly, several anthropogenic impact modules, based
502 on previous major works, were integrated into the VIC-5 macro-scale hydrological model: domestic,
503 industrial, energy, livestock and irrigation water withdrawals from both surface water and groundwater
504 as well as an integrated environmental flow requirement module and dam operation module. Global
505 gridded datasets on domestic, industrial, energy and livestock demand were developed separately and
506 used to force the VIC-WUR model.

507 Simulated national water withdrawals were in line with reported national annual withdrawals (R^2
508 adjusted > 0.8 ; both per sector as per source). However, the data-oriented methodology used to derive
509 sectoral water demands resulted in different withdrawal trends over time compared to other studies
510 (Shiklomanov, 2000; Huang et al., 2018). However, note that the model setup of VIC-WUR allows for
511 the evaluation of other sectoral water demand inputs, on various temporal aggregations. Terrestrial water
512 storage anomaly trends were well simulated (mean annual and inter-annual RMSE of 1.9 mm and 3.6

513 mm respectively), while groundwater exploitation was overestimated. Overestimated groundwater
514 depletion rates are likely related to an over-partitioning of water withdrawals to groundwater. The
515 implemented human impact modules increased simulated discharge performance (370 out of 462
516 stations), mostly due to the effects of reservoir operation.

517 An assessment of the effect of EFRs shows that, when one would adhere to these requirements, global
518 water withdrawals would be severely limited (39 %). This limitation is especially the case for
519 groundwater withdrawals, which, under the strict requirements used in our study, need to be reduced by
520 81 %.

521 VIC-WUR has potential for studying impacts of climate change and anthropogenic developments on
522 current and future water resources and sectoral specific-water scarcity. The additions presented here
523 make the VIC model more suited for fully-integrated worldwide water-resource assessments and
524 substantially decrease computation times compared to previous versions.

525 **5 Code availability**

526 All code for the VIC-WUR model is freely available at github.com/wur-wsg/VIC (tag VIC-WUR.2.0.0;
527 DOI 10.5281/zenodo.3399450) under the GNU General Public License, version 2 (GPL-2.0). VIC-
528 WUR documentation can be found at vicwur.readthedocs.io. The original VIC model is freely available
529 at github.com/UW-Hydro/VIC (tag VIC.5.0.1; DOI 10.5281/zenodo.267178) under the GNU General
530 Public License, version 2 (GPL-2.0). VIC documentation can be found at vic.readthedocs.io.
531 Documentation and scripts concerning inputs, configurations and analysis used in our study is freely
532 available at github.com/bramdr/VIC-WUR_support (tag VIC-WUR.2.0.0; DOI
533 10.5281/zenodo.3401411) under the GNU General Public License, version 3 (GPL-3.0).

534 **6 Appendix**

535 **6.1 Appendix A: VIC water and energy balance**

536 In VIC each sub-grid computes the water and energy balance individually (i.e. sub-grid do not exchange
537 water or energy between one another). For the water balance, incoming precipitation is partitioned

538 between evapotranspiration, surface and subsurface runoff, and soil water storage. Potential
539 evapotranspiration is based on the Penman-Monteith equation without the canopy resistance
540 (Shuttleworth, 1993). The actual evapotranspiration is calculated by two methods, based on whether the
541 land cover is vegetated or not (bare soil). Evapotranspiration of vegetation is constrained by stomatal,
542 architectural and aerodynamic resistances and is partitioned between canopy evaporation and
543 transpiration based on the intercepted water content of the canopy (Deardorff, 1978; Ducoudre et al.,
544 1993). Bare soil evaporation is constrained by the saturated area of the upper soil layer. The saturated
545 area is variable within the grid since (as the model name implies) the infiltration capacity of the soil is
546 assumed heterogeneous (Franchini and Pacciani, 1991). Saturated areas evaporate at the potential
547 evaporation rate while in unsaturated areas evaporation is limited. Surface runoff is produced by
548 precipitation over saturated areas. Precipitation over unsaturated areas infiltrates into the upper soil layer
549 and drains through the soil layers based on the gravitational hydraulic conductivity equations of Brooks
550 and Corey (1964). In the first and second layer water is available for transpiration, while the third layer
551 is assumed to be below the root zone. From the third layer baseflow is generated based on the non-linear
552 Arno conceptualization (Franchini and Pacciani, 1991). Baseflow increases linearly with soil moisture
553 content when the moisture content is low. At higher soil moisture contents the relation is non-linear,
554 representing subsurface storm-flows.

555 For the energy balance, incoming net radiation is partitioned between sensible, latent, and ground heat
556 fluxes and energy storage in the air below the canopy. The energy storage below the canopy is omitted
557 if it is considered negligible (e.g. the canopy surface is open or close to the ground). The latent heat flux
558 is determined by the evapotranspiration as calculated in the water balance. The sensible heat flux is
559 calculated based on the difference between the air and surface temperature and the ground heat flux is
560 calculated based on the difference between the soil and surface temperature. Since the incoming net
561 radiation is also a function of the surface temperature (specifically the outgoing longwave radiation),
562 the surface temperature is solved iteratively. Subsurface ground heat fluxes are calculated assuming an
563 exponential temperature profile between the surface and the bottom of the soil column, where the bottom
564 temperature is assumed constant. Later model developments included options for finite difference

565 solutions of the ground temperature profile (Cherkauer and Lettenmaier, 1999), spatial distribution of
566 soil temperatures (Cherkauer and Lettenmaier, 2003), a quasi-2-layer snow-pack snow model
567 (Andreadis et al., 2009), and blowing snow sublimation (Bowling et al., 2004).

568 **6.2 Appendix B: EFRs for surface and groundwater**

569 VIC-WUR used the Variable Monthly Flow (VMF) method (Pastor et al., 2014) to limit surface water
570 withdrawals. The VMF method (Pastor et al., 2014) calculates the EFRs for streamflow as a fraction of
571 the natural flow during high (Eq. A.1), intermediate (Eq. A.2) and low (Eq. A.3) flow periods. The
572 presumptive standard Gleeson and Richter (2018) is used to limit groundwater withdrawals (including
573 aquifer groundwater withdrawals). This standard calculates the EFRs for baseflow as 90 % of the natural
574 subsurface runoff through time (Eq. A.4). Here, daily instead of monthly EFRs were used to better
575 capture the monthly flow variability.

$$576 \quad EFR_{s,d} = 0.6 \cdot NF_{s,d} \quad \text{Eq. (A.1)}$$

$$577 \quad \text{where } NF_{s,d} \leq 0.4 \cdot NF_{s,y}$$

$$578 \quad EFR_{s,d} = 0.45 \cdot NF_{s,d} \quad \text{Eq. (A.2)}$$

$$579 \quad \text{where } 0.4 \cdot NF_{s,y} < NF_{s,d} \leq 0.8 \cdot NF_{s,y}$$

$$580 \quad EFR_{s,d} = 0.3 \cdot NF_{s,d} \quad \text{Eq. (A.3)}$$

$$581 \quad \text{where } NF_{s,d} > 0.8 \cdot NF_{s,y}$$

$$582 \quad EFR_{b,d} = 0.9 \cdot NF_{b,d} \quad \text{Eq. (A.4)}$$

583 Where $EFR_{s,d}$ is the daily EFRs for streamflow [$\text{m}^3 \text{s}^{-1}$], $EFR_{b,d}$ the daily EFRs for baseflow [$\text{m}^3 \text{s}^{-1}$],
584 $NF_{s,d}$ is the average natural daily streamflow [$\text{m}^3 \text{s}^{-1}$], and $NF_{s,y}$ is the average natural yearly streamflow
585 [$\text{m}^3 \text{s}^{-1}$], and $NF_{b,d}$ is the average natural daily baseflow [$\text{m}^3 \text{s}^{-1}$].

586 EFRs for streamflow and baseflow were based on VIC-WUR naturalized simulations between 1980 and
587 2010. Average natural daily flows were calculated as the interpolated multi-year monthly average flow
588 over the simulation period.

589 6.3 Appendix C: Dam operation scheme

590 VIC-WUR used a dam operation scheme based on Hanasaki et al. (2006). Target release (i.e. the
591 estimated optimal release) was calculated at the start of the operational year. The operational year starts
592 at the month where the inflow drops below the average annual inflow, and thus the storage should be at
593 its desired maximum. The scheme distinguished between two dam types: (1) dams that did not account
594 for water demands downstream (e.g. hydropower dams or flood control) and (2) dams that did account
595 for water demands downstream (e.g. irrigation dams). The original scheme of Hanasaki et al. (2006)
596 also accounts for EFRs, which were fixed at half the annual mean inflow. Other studies lowered the
597 requirements to a tenth of the mean annual inflow, increasing irrigation availability and preventing
598 excessive releases (Biemans et al., 2011; Voisin et al., 2013). In our study the original dam operation
599 scheme was adapted slightly to account for monthly varying EFRs.

600 For dams that did not account for demands, the initial release was set at the mean annual inflow corrected
601 by the variable EFRs (Eq. A.5). For dams that did account for demands, the initial release was increased
602 during periods of higher water demand. If demands were relatively high compared to the annual inflow,
603 the release was corrected by the demand relative to the mean demand (Eq. A.6). If demands were
604 relatively low compared to the annual inflow, release was corrected based on the actual water demand
605 (Eq. A.7).

606

$$607 \quad R'_m = EFR_{s,m} + (I_y - EFR_{s,y}) \quad \text{Eq. (A.5)}$$

$$608 \quad \text{where } D_y = 0$$

$$609 \quad R'_m = EFR_{s,m} + (I_y - EFR_{s,y}) * \frac{D_m}{D_y} \quad \text{Eq. (A.6)}$$

$$610 \quad \text{where } D_y > 0 \text{ and } D_y > (I_y - EFR_{s,y})$$

$$611 \quad R'_m = EFR_{s,m} + (I_y - EFR_{s,y}) - D_y + D_m \quad \text{Eq. (A.7)}$$

$$612 \quad \text{where } D_y > 0 \text{ and } D_y \leq (I_y - EFR_{s,y})$$

613 Where R'_m is the initial monthly target release [$\text{m}^3 \text{s}^{-1}$], $EFR_{s,m}$ is the average monthly EFR for
 614 streamflow demand [$\text{m}^3 \text{s}^{-1}$], I_y is the average yearly inflow [$\text{m}^3 \text{s}^{-1}$], $EFR_{s,y}$ is the average yearly EFR
 615 for streamflow [$\text{m}^3 \text{s}^{-1}$], D_m is the average monthly water demand [$\text{m}^3 \text{s}^{-1}$] and D_y is the average yearly
 616 water demand [$\text{m}^3 \text{s}^{-1}$].

617 As in Hanasaki et al. (2006), the initial target release was adjusted based on storage and capacity. Target
 618 release was adjusted to compensate differences between the current storage and the desired maximum
 619 storage (Eq. A.8). Target release was additionally adjusted if the storage capacity is relatively low
 620 compared to the annual inflow, and unable to store large portions of the inflow for later release (Eq.
 621 A.9).

$$622 \quad R_m = k \cdot R'_m \quad \text{Eq. (A.8)}$$

623 where $c \geq 0.5$

$$624 \quad R_m = \left(\frac{c}{0.5}\right)^2 \cdot k \cdot R'_m + \left\{1 - \left(\frac{c}{0.5}\right)^2\right\} \cdot I_m \quad \text{Eq. (A.9)}$$

625 where $0 \leq c \leq 0.5$

626 Where I_y is the average monthly inflow [$\text{m}^3 \text{s}^{-1}$], c the capacity parameter [-] calculated as the storage
 627 capacity divided by the mean annual inflow and k the storage parameter [-] calculated as current storage
 628 divided by the desired maximum storage. The desired maximum storage was set at 85 % of the storage
 629 capacity as recommended by Hanasaki et al. (2006).

630 Water inflow, demand and EFRs were estimated based on the average of the past five years. Water
 631 demands were based on the water demands of downstream cells. Only a fraction of water demands were
 632 taken into account, based on the fraction of discharge the dam controlled. For example: if a dam
 633 controlled 70 % of the discharge of a downstream cell, than 70 % of its demands were taken into account.
 634 Fractions smaller than 25 % were ignored.

635 The original dam operation scheme of Hanasaki et al. (2006) was shown to produce excessively high
 636 discharge events due to overflow releases (Masaki et al., 2018b). These overflow releases occurred due
 637 to a mismatch between the expected and actual inflow. In our study, dam release was increased during

638 high-storage events to prevent overflow and accompanying high discharge events. If dam storage was
 639 above the desired maximum storage, target dam release was increased to negate the difference (Eq.
 640 A.10). If dam storage was below the desired minimum storage, release is decreased (Eq. A.11). Dam
 641 release was adjusted exponentially based on the relative storage difference: small storage differences
 642 were only corrected slightly, but if the dam was close to overflowing or emptying, the difference was
 643 corrected strongly.

$$644 \quad R_a = R_m + \frac{(S-C\alpha)}{\gamma} \cdot \left(\frac{\frac{S}{C} - \alpha}{1-\alpha} \right)^b \quad \text{Eq. (A.10)}$$

645 *where $S > C\alpha$*

$$646 \quad R_a = R_m + \frac{(S-C(1-\alpha))}{\gamma} \cdot \left(\frac{(1-\alpha) - \frac{S}{C}}{1-\alpha} \right)^b \quad \text{Eq. (A.11)}$$

647 *where $S < C(1 - \alpha)$*

648 Where R_a is the actual dam release [$\text{m}^3 \text{s}^{-1}$], S the dam storage capacity [m^3], α the fraction of the capacity
 649 that is the desired maximum [-], β the exponent determining the correction increase [-] and γ the
 650 parameter determining the period when the release is corrected [s^{-1}]. In testing the exponent and period
 651 were tuned to 0.6 and 5 days respectively.

652 **6.4 Appendix D: Water demand**

653 **6.4.1 Fitting and validation data**

654 Data on irrigation, domestic and industrial water withdrawals were based on the AQUASTAT database
 655 (FAO, 2016), EUROSTAT database (EC, 2019) and United Nations World Water Development Report
 656 (Connor, 2015). Data on GDP per capita and GVA was abstracted from the Maddison Project Database
 657 2018 (Bolt et al., 2018), Penn World Table 9.0 (Feenstra et al., 2015) and World Bank Development
 658 Indicators (World bank, 2010).

659 Available data for domestic and industrial withdrawals were divided into a dataset used for parameter
 660 fitting (80 %) and a dataset used for validation (20 %). Domestic water demands were estimated for
 661 each United Nations sub-region, and thus data was divided per sub-region to ensure a good global

662 coverage of data. In the same manner industrial water demand were divided per country. In case there
663 is only a single data point, the data was added to both the fitting and validation data.

664 **6.4.2 Irrigation sector**

665 Conventional irrigation demands were calculated when soil moisture contents drop below the critical
666 threshold where evapotranspiration will be limited. Demands were set to relieve water stress (Eq. A.12).
667 Paddy irrigation demands were set to always keep the soil moisture content of the upper soil layer
668 saturated (Eq. A.13), similar to Hanasaki et al. (2008a) and Wada et al. (2014). For paddy irrigation, the
669 saturated hydraulic conductivity of the upper soil layer was reduced by its cubed root to simulate
670 puddling practices, as recommended by the CROPWAT model (Smith, 1996). Total irrigation demands
671 were adjusted by the irrigation efficiency (Eq. A.14). Paddy irrigation used an irrigation efficiency of 1
672 since the water losses were already incorporated in the water demand calculation.

$$673 \quad ID'_{conventional} = (W_{cr,1} + W_{cr,2}) - (W_1 + W_2) \quad \text{Eq. (A.12)}$$

$$674 \quad \text{where } W_1 + W_2 < W_{cr,1} + W_{cr,2}$$

$$675 \quad ID'_{paddy} = W_{max,1} - W_1 \quad \text{Eq. (A.13)}$$

$$676 \quad \text{where } W_1 < W_{max,1}$$

$$677 \quad ID = ID' * IE \quad \text{Eq. (A.14)}$$

678 Where $ID'_{conventional}$ is the conventional crop irrigation demand [mm], ID'_{paddy} is the paddy crop irrigation
679 demand [mm], ID is the total irrigation demand [mm], W_1 and W_2 are the soil moisture contents of the
680 first and second soil layer respectively [mm], W_{cr} is the critical soil moisture content [mm], W_{max} the
681 maximum soil moisture content [mm], and IE is the irrigation efficiency [mm mm⁻¹].

682 **6.4.3 Domestic sector**

683 Domestic water demands were represented by using a sigmoid curve for the calculation of structural
684 domestic water demands (Eq.A.15) and a efficiency rate for the calculation of water-use efficiency
685 increases (Eq. A.16). These equations differ slightly from Alcamo et al. (2003) since our study used the
686 base 10 logarithms of GDP and water withdrawals per capita as they provided a better fit.

687
$$DSW_y = DSW_{min} + (DSW_{max} - DSW_{min}) * \frac{1}{1 + e^{-f(GDP_y - o)}}$$
 Eq. (A.15)

688
$$DW_y = 10^{DSW_y} \cdot TE^{y - y_{base}}$$
 Eq. (A.16)

689 Where DSW is the yearly structural domestic withdrawal [$\log_{10} \text{ m}^3 \text{ cap}^{-1}$], DW the yearly domestic
 690 withdrawal [$\text{m}^3 \text{ cap}^{-1}$], DW_{min} the minimum structural domestic withdrawal [$\log_{10} \text{ m}^3 \text{ cap}^{-1}$], DW_{max} the
 691 maximum structural domestic withdrawal (without technological improvement) [$\log_{10} \text{ m}^3 \text{ cap}^{-1}$], GDP
 692 the yearly gross domestic product [$\log_{10} \text{ USD}_{\text{equivalent}} \text{ cap}^{-1}$], f [-] and o [$\log_{10} \text{ USD}_{\text{equivalent}}$] the
 693 parameters that determine the range and steepness of the sigmoid curve, y the year index, TE the
 694 technological efficiency rate [-], and y_{base} the base year (taken to be 1980).

695 DW_{min} was set at $7.5 \text{ l cap}^{-1} \text{ d}^{-1}$ based on the World Health Organisation standard (Reed and Reed, 2013),
 696 DW_{max} was estimated at around $450 \text{ l cap}^{-1} \text{ y}^{-1}$ based on a global curve fit, and TE was set at 0.995, 0.99,
 697 and 0.98 for developing, transition and developed countries respectively (United Nations development
 698 status classification) based on Flörke et al. (2013). Curve parameters f and o were estimated for the 23
 699 United Nations sub-regions based on the GDP per capita and domestic water withdrawal data. In case
 700 insufficient data was available to calculate parameters values, regional (4 sub-regions) or global (4 sub-
 701 regions) parameter estimates were used.

702 **6.4.4 Industrial sector**

703 Industrial water demands were represented by using a linear formula for the calculation of structural
 704 industrial water demands (Eq. A.17) and a efficiency rate for the calculation of water-use efficiency
 705 increases (Eq. A.18).

706
$$ISW_y = ISW_{int} \cdot GVA_y$$
 Eq. (A.17)

707
$$IW_y = ISW_y \cdot TE^{y - y_{base}}$$
 Eq. (A.18)

708 Where ISW is the yearly structural industrial withdrawal [m^3], IW_{int} the country specific industrial water
 709 intensity [$\text{m USD}_{\text{equivalent}}^{-1}$], IW the yearly industrial withdrawal [m^3], GVA the yearly gross value added
 710 by industry [$\text{USD}_{\text{equivalent}}$], y the year index, y_{base} the base year (taken to be the year when the industrial
 711 water intensity is determined), and TE the technological efficiency rate [-].

712 TE was set at 0.976 and 1 for OECD and non-OECD countries respectively before the year 1980, 0.976
713 between the years 1980 and 2000 and 0.99 after the year 2000 based on Flörke et al. (2013). Industrial
714 water intensities were estimated for the 246 United Nations countries based on the GVA and industrial
715 water withdrawal data. In case insufficient data was available to calculate the industrial water intensities,
716 either sub-regional (56 countries), regional (17 countries) or global (9 countries) intensities estimates
717 were used.

718 **6.4.5 Energy sector**

719 For each thermoelectric power plant the water intensity was combined with their generation to calculate
720 the water demands (Eq. A.19). Actual generation is estimated by adjusting the installed generation
721 capacity by 46 % for fossil, 72 % for nuclear and 56 % for biomass power plants (based on EIA national
722 annual generation data (EIA, 2013))

$$723 \quad EW_y = EW_{int} \cdot G_y \quad \text{Eq. (A.19)}$$

724 Where EW is the yearly energy withdrawal [m^3], EW_{int} the energy water intensity [$m^3 \text{ MWh}^{-1}$], G the
725 yearly generation for each plant [MWh], and y the year index.

726 The energy water demands were subtracted from the industrial water demands at the location of each
727 power plant. In cases where the grid cell industrial water demand was less than the energy water demand,
728 national industrial water demands were lowered. In cases where even the national industrial water
729 demands were less than the national energy water demand (3 countries), the energy water demands were
730 lowered instead. Energy demands were lowered until 10 % of the national industrial water demand
731 remains, to ensure some spatial coverage of industrial and energy water demands.

732 **6.4.6 Livestock sector**

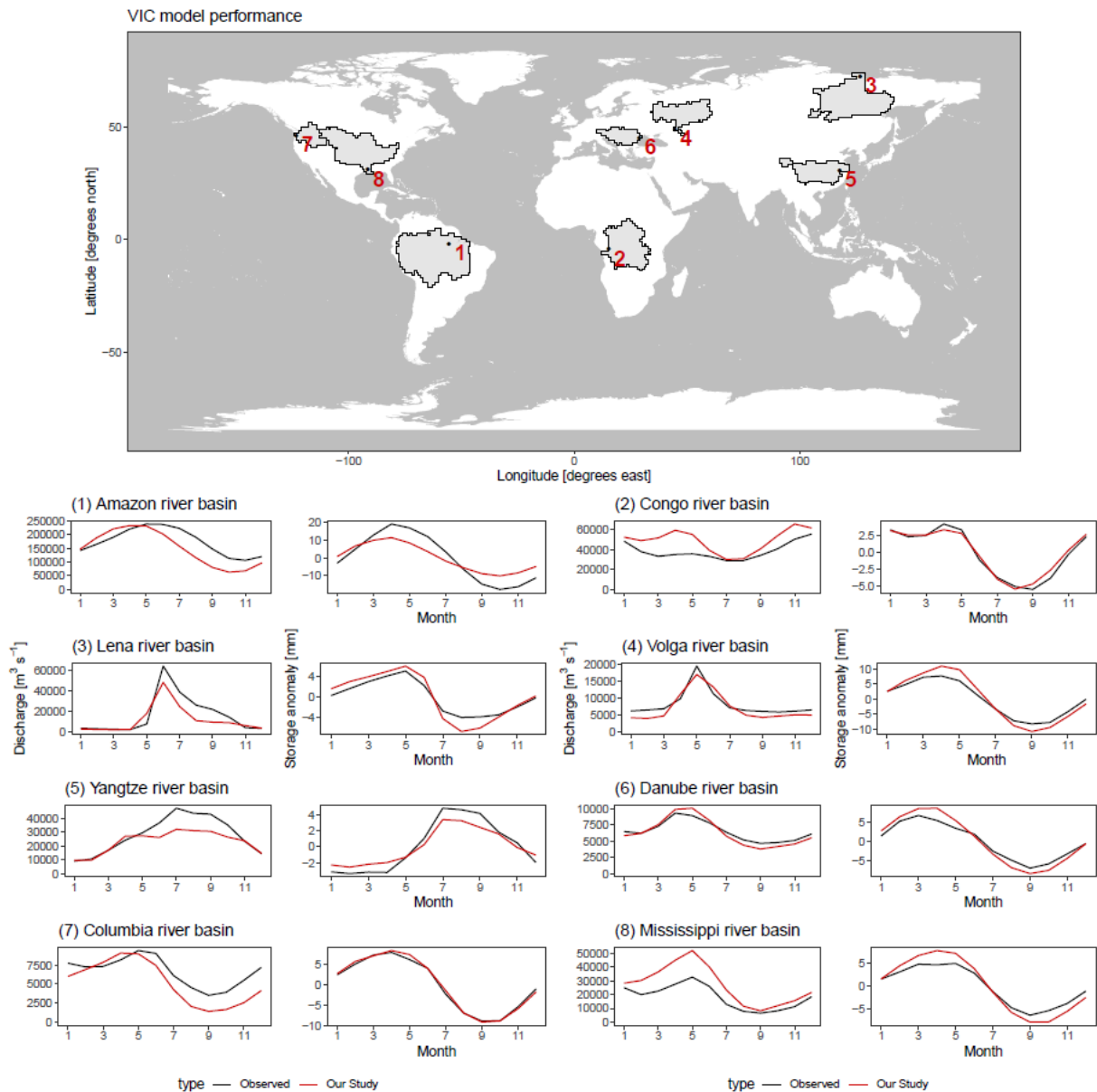
733 Livestock water demands were estimated by combining the livestock population with the water
734 requirements for each livestock variety (Eq. A.20).

$$735 \quad LW_y = LW_{int} \cdot L \quad \text{Eq. (A.20)}$$

736 Where LW is the yearly livestock withdrawal [m^3], LW_{int} the livestock water intensity [m^3 livestock $^{-1}$],
737 L the livestock number for each variety [livestock].

738 **6.5 Appendix E: General performance**

739 VIC-WUR monthly discharge and monthly terrestrial total water storage anomalies were compared with
740 observations from the GRDC dataset (GRDC, 2003) and GRACE satellite dataset (NASA, 2002) for
741 eight major river basins (not included in the main text). Discharge stations were selected if the upstream
742 area was larger than 10000 m^2 , matched the simulated upstream area at the station location,): Amazon,
743 Congo, Lena, Volga, Yangtze, Danube, Columbia and Mississippi river basins. A 300km gaussian filter
744 has been applied to the total water storage simulation data (similar to Long et al. (2015)).



745

746 **Figure A1: Comparison between simulated and observed discharge and terrestrial total water storage anomalies.**
 747 **Figures indicate multi-year averages of human-impacted simulations (red) and observations (black).**

748 **7 Author contribution**

749 Bram Droppers and Wietse H.P. Fransen developed and tested the model additions introduced in VIC-
 750 WUR. Bram Droppers generated and analysed the results. Michelle T.H. van Vliet, Bart Nijssen and
 751 Fulco Ludwig provided overall oversight and guidance. Bram Droppers prepared the manuscript with
 752 contributions from all co-authors.

753 **8 Competing interests**

754 The authors declare that they have no conflict of interest.

755 **9 Acknowledgements**

756 We would like to thank Rik Leemans for his guidance and detailed comments. We would like to thank
757 the Wageningen Institute for Environment and Climate Research (WIMEK) for providing funding for
758 our research.

759 **10 References**

- 760 Abdulla, F. A., Lettenmaier, D. P., Wood, E. F., and Smith, J. A.: Application of a macroscale hydrologic
761 model to estimate the water balance of the Arkansas Red River basin, *J Geophys Res-Atmos*,
762 101, 7449-7459, 10.1029/95jd02416, 1996.
- 763 Alcamo, J., Döll, P., Kaspar, F., and Siebert, S.: Global change and global scenarios of water use and
764 availability: an application of WaterGAP1.0, Center for environmental systems research,
765 University of Kassel, Kassel, Germany, 96, 1997.
- 766 Alcamo, J., Döll, P., Henrichs, T., Kaspar, F., Lehner, B., Rosch, T., and Siebert, S.: Development and
767 testing of the WaterGAP 2 global model of water use and availability, *Hydrolog Sci J*, 48, 317-
768 337, 10.1623/hysj.48.3.317.45290, 2003.
- 769 Allen, R. G., Pereira, L. S., Raes, D., and Smith, M.: Crop Evapotranspiration - Guidelines for
770 computing crop water requirements, Food and Agricultural Organisation, Rome, Italy, 326,
771 1998.
- 772 Andreadis, K. M., Storck, P., and Lettenmaier, D. P.: Modeling snow accumulation and ablation
773 processes in forested environments, *Water Resour Res*, 45, 10.1029/2008wr007042, 2009.
- 774 Babel, M. S., Das Gupta, A., and Pradhan, P.: A multivariate econometric approach for domestic water
775 demand modeling: An application to Kathmandu, Nepal, *Water Resour Manag*, 21, 573-589,
776 10.1007/s11269-006-9030-6, 2007.
- 777 Bazilian, M., Rogner, H., Howells, M., Hermann, S., Arent, D., Gielen, D., Steduto, P., Mueller, A.,
778 Komor, P., Tol, R. S. J., and Yumkella, K. K.: Considering the energy, water and food nexus:
779 Towards an integrated modelling approach, *Energ Policy*, 39, 7896-7906,
780 10.1016/j.enpol.2011.09.039, 2011.
- 781 Best, M. J., Pryor, M., Clark, D. B., Rooney, G. G., Essery, R. L. H., Menard, C. B., Edwards, J. M.,
782 Hendry, M. A., Porson, A., Gedney, N., Mercado, L. M., Sitch, S., Blyth, E., Boucher, O., Cox,
783 P. M., Grimmond, C. S. B., and Harding, R. J.: The Joint UK Land Environment Simulator

784 (JULES), model description - Part 1: Energy and water fluxes, *Geosci Model Dev*, 4, 677-699,
785 10.5194/gmd-4-677-2011, 2011.

786 Biemans, H., Haddeland, I., Kabat, P., Ludwig, F., Hutjes, R. W. A., Heinke, J., von Bloh, W., and
787 Gerten, D.: Impact of reservoirs on river discharge and irrigation water supply during the 20th
788 century, *Water Resour Res*, 47, 10.1029/2009wr008929, 2011.

789 Bijl, D. L., Bogaart, P. W., Dekker, S. C., and van Vuuren, D. P.: Unpacking the nexus: Different spatial
790 scales for water, food and energy, *Global Environ Chang*, 48, 22-31,
791 10.1016/j.gloenvcha.2017.11.005, 2018.

792 Bolt, J., Inklaar, R., de Jong, H., and van Zanden, J. L.: Rebasings 'Maddison': New income comparisons
793 and the shape of long-run economic developments, University of Groningen, Groningen, the
794 Netherlands, 69, 2018.

795 Bondeau, A., Smith, P. C., Zaehle, S., Schaphoff, S., Lucht, W., Cramer, W., Gerten, D., Lotze-Campen,
796 H., Muller, C., Reichstein, M., and Smith, B.: Modelling the role of agriculture for the 20th
797 century global terrestrial carbon balance, *Global Change Biol*, 13, 679-706, 10.1111/j.1365-
798 2486.2006.01305.x, 2007.

799 Bowling, L. C., Pomeroy, J. W., and Lettenmaier, D. P.: Parameterization of blowing-snow sublimation
800 in a macroscale hydrology model, *J Hydrometeorol*, 5, 745-762, 10.1175/1525-
801 7541(2004)005<0745:Pobsia>2.0.Co;2, 2004.

802 Brooks, R. H., and Corey, A. T.: Hydraulic properties of porous media, Colorado state university, Fort
803 Collins, Colorado, 27, 1964.

804 Brouwer, C., Prins, K., and Heibloem, M.: Irrigation water management: Irrigation scheduling, Food
805 and Agricultural Organisation, Rome, Italy, 66, 1989.

806 Calder, I. R.: Hydrologic effects of land use change, in: Handbook of hydrology, edited by: Maidment,
807 D. R., McGraw-Hill, New York, 13, 1993.

808 Carpenter, S. R., Stanley, E. H., and Vander Zanden, M. J.: State of the World's Freshwater Ecosystems:
809 Physical, Chemical, and Biological Changes, *Annu Rev Env Resour*, 36, 75-99,
810 10.1146/annurev-environ-021810-094524, 2011.

811 Carter, A. J., and Scholes, R. J.: Generating a global database of soil properties, IGBP Data and
812 Information Services, Potsdam, Germany, 10, 1999.

813 Chateau, J., Dellink, R., and Lanzi, E.: An overview of the OECD ENV-linkages model, Organisation
814 for economic co-operation and development, 43, 2014.

815 Chegwidan, O. S., Nijssen, B., Rupp, D. E., Arnold, J. R., Clark, M. P., Hamman, J. J., Kao, S.-C.,
816 Mao, Y., Mizukami, N., Mote, P. W., Pan, M., Pytlak, E., and Xiao, M.: How Do Modeling
817 Decisions Affect the Spread Among Hydrologic Climate Change Projections? Exploring a Large
818 Ensemble of Simulations Across a Diversity of Hydroclimates, *Earth's Future*, 7, 623-637,
819 10.1029/2018ef001047, 2019.

820 Cherkauer, K. A., and Lettenmaier, D. P.: Hydrologic effects of frozen soils in the upper Mississippi
821 River basin, *J Geophys Res-Atmos*, 104, 19599-19610, 10.1029/1999jd900337, 1999.

822 Cherkauer, K. A., and Lettenmaier, D. P.: Simulation of spatial variability in snow and frozen soil, *J*
823 *Geophys Res-Atmos*, 108, 10.1029/2003jd003575, 2003.

824 Connor, R.: Water for a sustainable world, United Nations Educational, Scientific and Cultural
825 Organisation, Paris, France, 139, 2015.

826 Cosby, B. J., Hornberger, G. M., Clapp, R. B., and Ginn, T. R.: A Statistical Exploration of the
827 Relationships of Soil-Moisture Characteristics to the Physical-Properties of Soils, *Water Resour*
828 *Res*, 20, 682-690, 10.1029/WR020i006p00682, 1984.

829 de Graaf, I. E. M., van Beek, R. L. P. H., Gleeson, T., Moosdorf, N., Schmitz, O., Sutanudjaja, E. H.,
830 and Bierkens, M. F. P.: A global-scale two-layer transient groundwater model: Development
831 and application to groundwater depletion, *Adv Water Resour*, 102, 53-67,
832 10.1016/j.advwatres.2017.01.011, 2017.

833 Deardorff, J. W.: Efficient Prediction of Ground Surface-Temperature and Moisture, with Inclusion of
834 a Layer of Vegetation, *J Geophys Res-Oceans*, 83, 1889-1903, 10.1029/JC083iC04p01889,
835 1978.

836 Döll, P., Fiedler, K., and Zhang, J.: Global-scale analysis of river flow alterations due to water
837 withdrawals and reservoirs, *Hydrol Earth Syst Sc*, 13, 2413-2432, 2009.

838 Döll, P., Hoffmann-Dobrev, H., Portmann, F. T., Siebert, S., Eicker, A., Rodell, M., Strassberg, G., and
839 Scanlon, B. R.: Impact of water withdrawals from groundwater and surface water on continental
840 water storage variations, *J Geodyn*, 59-60, 143-156, 10.1016/j.jog.2011.05.001, 2012.

841 Döll, P., Müller Schmied, H., Schuh, C., Portmann, F. T., and Eicker, A.: Global-scale assessment of
842 groundwater depletion and related groundwater abstractions: Combining hydrological modeling
843 with information from well observations and GRACE satellites, *Water Resour Res*, 50, 5698-
844 5720, 10.1002/2014wr015595, 2014.

845 Döll, P., Douville, H., Guntner, A., Müller Schmied, H., and Wada, Y.: Modelling Freshwater Resources
846 at the Global Scale: Challenges and Prospects, *Surv Geophys*, 37, 195-221, 10.1007/s10712-
847 015-9343-1, 2016.

848 Ducoudre, N. I., Laval, K., and Perrier, A.: Sechiba, a New Set of Parameterizations of the Hydrologic
849 Exchanges at the Land Atmosphere Interface within the Lmd Atmospheric General-Circulation
850 Model, *J Climate*, 6, 248-273, 10.1175/1520-0442(1993)006<0248:Sansop>2.0.Co;2, 1993.

851 Famiglietti, J. S.: The global groundwater crisis, *Nat Clim Change*, 4, 945-948, 10.1038/nclimate2425,
852 2014.

853 Feenstra, R. C., Inklaar, R., and Timmer, M. P.: The Next Generation of the Penn World Table, *Am*
854 *Econ Rev*, 105, 3150-3182, 10.1257/aer.20130954, 2015.

855 Flörke, M., and Alcamo, J.: European outlook on water use, Centre for environmental systems research,
856 Kassel, 86, 2004.

857 Flörke, M., Kynast, E., Barlund, I., Eisner, S., Wimmer, F., and Alcamo, J.: Domestic and industrial
858 water uses of the past 60 years as a mirror of socio-economic development: A global simulation
859 study, *Global Environ Chang*, 23, 144-156, 10.1016/j.gloenvcha.2012.10.018, 2013.

860 Franchini, M., and Pacciani, M.: Comparative-Analysis of Several Conceptual Rainfall Runoff Models,
861 *J Hydrol*, 122, 161-219, 10.1016/0022-1694(91)90178-K, 1991.

862 Frenken, K., and Gillet, V.: Irrigation water requirement and water withdrawal by country, Food and
863 agricultural organisation, Rome, Italy, 264, 2012.

864 Gerten, D., Hoff, H., Rockstrom, J., Jagermeyr, J., Kummu, M., and Pastor, A. V.: Towards a revised
865 planetary boundary for consumptive freshwater use: role of environmental flow requirements,
866 *Curr Opin Env Sust*, 5, 551-558, 10.1016/j.cosust.2013.11.001, 2013.

867 Gilbert, M., Nicolas, G., Cinardi, G., Van Boeckel, T. P., Vanwambeke, S. O., Wint, G. R. W., and
868 Robinson, T. P.: Global distribution data for cattle, buffaloes, horses, sheep, goats, pigs, chickens
869 and ducks in 2010, *Sci Data*, 5, 10.1038/sdata.2018.227, 2018.

870 Gleeson, T., and Richter, B.: How much groundwater can we pump and protect environmental flows
871 through time? Presumptive standards for conjunctive management of aquifers and rivers, *River*
872 *Res Appl*, 34, 83-92, 10.1002/rra.3185, 2018.

873 Gleick, P. H., Cooley, H., Katz, D., Lee, E., Morrison, J., Meena, P., Samulon, A., and Wolff, G. H.:
874 The world's water 2006-2007: The biennial report on freshwater resources, Island Press,
875 Washington, 392 pp., 2013.

876 Goldewijk, K. K., Beusen, A., Doelman, J., and Stehfest, E.: Anthropogenic land use estimates for the
877 Holocene - HYDE 3.2, *Earth Syst Sci Data*, 9, 927-953, 10.5194/essd-9-927-2017, 2017.

878 Goldstein, R., and Smith, W.: U.S. water consumption for power production - the next half century,
879 Electric power research institute, California, United States, 57, 2002.

880 Grill, G., Lehner, B., Thieme, M., Geenen, B., Tickner, D., Antonelli, F., Babu, S., Borrelli, P., Cheng,
881 L., Crochetiere, H., Macedo, H. E., Filgueiras, R., Goichot, M., Higgins, J., Hogan, Z., Lip, B.,
882 McClain, M. E., Meng, J., Mulligan, M., Nilsson, C., Olden, J. D., Opperman, J. J., Petry, P.,
883 Liermann, C. R., Saenz, L., Salinas-Rodriguez, S., Schelle, P., Schmitt, R. J. P., Snider, J., Tan,
884 F., Tockner, K., Valdujo, P. H., van Soesbergen, A., and Zarfl, C.: Mapping the world's free-
885 flowing rivers, *Nature*, 569, 215+, 10.1038/s41586-019-1111-9, 2019.

886 Grobicki, A., Huidobro, P., Galloni, S., Asano, T., and Delgau, K. F.: Water, a shared responsibility
887 (chapter 8), United Nations Educational, Scientific and Cultural Organisation, Paris, France,
888 601, 2005.

889 Haddeland, I., Lettenmaier, D. P., and Skaugen, T.: Effects of irrigation on the water and energy balances
890 of the Colorado and Mekong river basins, *J Hydrol*, 324, 210-223,
891 10.1016/j.jhydrol.2005.09.028, 2006a.

892 Haddeland, I., Skaugen, T., and Lettenmaier, D. P.: Anthropogenic impacts on continental surface water
893 fluxes, *Geophys Res Lett*, 33, 10.1029/2006gl026047, 2006b.

894 Hagemann, S., and Gates, L. D.: Validation of the hydrological cycle of ECMWF and NCEP reanalyses
895 using the MPI hydrological discharge model, *J Geophys Res-Atmos*, 106, 1503-1510,
896 10.1029/2000jd900568, 2001.

897 Hamlet, A. F., and Lettenmaier, D. P.: Effects of climate change on hydrology and water resources in
898 the Columbia River basin, *J Am Water Resour As*, 35, 1597-1623, DOI 10.1111/j.1752-
899 1688.1999.tb04240.x, 1999.

900 Hamman, J., Nijssen, B., Brunke, M., Cassano, J., Craig, A., DuVivier, A., Hughes, M., Lettenmaier,
901 D. P., Maslowski, W., Osinski, R., Roberts, A., and Zeng, X. B.: Land Surface Climate in the
902 Regional Arctic System Model, *J Climate*, 29, 6543-6562, 10.1175/Jcli-D-15-0415.1, 2016.

903 Hamman, J., Nijssen, B., Roberts, A., Craig, A., Maslowski, W., and Osinski, R.: The coastal streamflow
904 flux in the Regional Arctic System Model, *J Geophys Res-Oceans*, 122, 1683-1701,
905 10.1002/2016jc012323, 2017.

906 Hamman, J. J., Nijssen, B., Bohn, T. J., Gergel, D. R., and Mao, Y. X.: The Variable Infiltration Capacity
907 model version 5 (VIC-5): infrastructure improvements for new applications and reproducibility,
908 *Geosci Model Dev*, 11, 3481-3496, 10.5194/gmd-11-3481-2018, 2018.

909 Hanasaki, N., Kanae, S., and Oki, T.: A reservoir operation scheme for global river routing models, *J*
910 *Hydrol*, 327, 22-41, 10.1016/j.jhydrol.2005.11.011, 2006.

911 Hanasaki, N., Kanae, S., Oki, T., Masuda, K., Motoya, K., Shirakawa, N., Shen, Y., and Tanaka, K.: An
912 integrated model for the assessment of global water resources Part 1: Model description and
913 input meteorological forcing, *Hydrol Earth Syst Sc*, 12, 1007-1025, 10.5194/hess-12-1007-
914 2008, 2008a.

915 Hanasaki, N., Kanae, S., Oki, T., Masuda, K., Motoya, K., Shirakawa, N., Shen, Y., and Tanaka, K.: An
916 integrated model for the assessment of global water resources Part 2: Applications and
917 assessments, *Hydrol Earth Syst Sc*, 12, 1027-1037, 10.5194/hess-12-1027-2008, 2008b.

918 Hanasaki, N., Yoshikawa, S., Pokhrel, Y., and Kanae, S.: A global hydrological simulation to specify
919 the sources of water used by humans, *Hydrol Earth Syst Sc*, 22, 789-817, 10.5194/hess-22-789-
920 2018, 2018.

921 Hansen, M. C., Defries, R. S., Townshend, J. R. G., and Sohlberg, R.: Global land cover classification
922 at 1km spatial resolution using a classification tree approach, *Int J Remote Sens*, 21, 1331-1364,
923 Doi 10.1080/014311600210209, 2000.

924 Harding, R., Best, M., Blyth, E., Hagemann, S., Kabat, P., Tallaksen, L. M., Warnaars, T., Wiberg, D.,
925 Weedon, G. P., Lanen, H. v., Ludwig, F., and Haddeland, I.: WATCH: Current Knowledge of
926 the Terrestrial Global Water Cycle, *J Hydrometeorol*, 12, 1149-1156, 10.1175/jhm-d-11-024.1,
927 2011.

928 Hejazi, M., Edmonds, J., Clarke, L., Kyle, P., Davies, E., Chaturvedi, V., Wise, M., Patel, P., Eom, J.,
929 Calvin, K., Moss, R., and Kim, S.: Long-term global water projections using six socioeconomic
930 scenarios in an integrated assessment modeling framework, *Technol Forecast Soc*, 81, 205-226,
931 10.1016/j.techfore.2013.05.006, 2014.

932 Huang, Z., Hejazi, M., Li, X., Tang, Q., Vernon, C., Leng, G., Liu, Y., Döll, P., Eisner, S., Gerten, D.,
933 Hanasaki, N., and Wada, Y.: Reconstruction of global gridded monthly sectoral water
934 withdrawals for 1971–2010 and analysis of their spatiotemporal patterns, *Hydrol. Earth Syst.*
935 *Sci.*, 22, 2117-2133, 10.5194/hess-22-2117-2018, 2018.

936 Jägermeyr, J., Pastor, A., Biemans, H., and Gerten, D.: Reconciling irrigated food production with
937 environmental flows for Sustainable Development Goals implementation, *Nature*
938 *Communications*, 8, 15900, 10.1038/ncomms15900, 2017.

939 Kim, S. H., Hejazi, M., Liu, L., Calvin, K., Clarke, L., Edmonds, J., Kyle, P., Patel, P., Wise, M., and
940 Davies, E.: Balancing global water availability and use at basin scale in an integrated assessment
941 model, *Climatic Change*, 136, 217-231, 10.1007/s10584-016-1604-6, 2016.

942 Konikow, L. F.: Contribution of global groundwater depletion since 1900 to sea-level rise, *Geophys Res*
943 *Lett*, 38, 10.1029/2011gl048604, 2011.

944 Krinner, G., Viovy, N., de Noblet-Ducoudre, N., Ogee, J., Polcher, J., Friedlingstein, P., Ciais, P., Sitch,
945 S., and Prentice, I. C.: A dynamic global vegetation model for studies of the coupled atmosphere-
946 biosphere system, *Global Biogeochem Cy*, 19, 10.1029/2003gb002199, 2005.

947 Lehner, B., Liermann, C. R., Revenga, C., Vorosmarty, C., Fekete, B., Crouzet, P., Döll, P., Endejan,
948 M., Frenken, K., Magome, J., Nilsson, C., Robertson, J. C., Rodel, R., Sindorf, N., and Wisser,
949 D.: High-resolution mapping of the world's reservoirs and dams for sustainable river-flow
950 management, *Front Ecol Environ*, 9, 494-502, 10.1890/100125, 2011.

951 Liang, X., Lettenmaier, D. P., Wood, E. F., and Burges, S. J.: A Simple Hydrologically Based Model of
952 Land-Surface Water and Energy Fluxes for General-Circulation Models, *J Geophys Res-Atmos*,
953 99, 14415-14428, 10.1029/94jd00483, 1994.

954 Lohmann, D., Nolte-Holube, R., and Raschke, E.: A large-scale horizontal routing model to be coupled
955 to land surface parametrization schemes, *Tellus A*, 48, 708-721, 10.1034/j.1600-0870.1996.t01-
956 3-00009.x, 1996.

957 Lohmann, D., Raschke, E., Nijssen, B., and Lettenmaier, D. P.: Regional scale hydrology: I. Formulation
958 of the VIC-2L model coupled to a routing model, *Hydrolog Sci J*, 43, 131-141,
959 10.1080/02626669809492107, 1998a.

960 Lohmann, D., Raschke, E., Nijssen, B., and Lettenmaier, D. P.: Regional scale hydrology: II.
961 Application of the VIC-2L model to the Weser River, Germany, *Hydrolog Sci J*, 43, 143-158,
962 10.1080/02626669809492108, 1998b.

963 Long, D., Yang, Y., Wada, Y., Hong, Y., Liang, W., Chen, Y., Yong, B., Hou, A., Wei, J., and Chen,
964 L.: Deriving scaling factors using a global hydrological model to restore GRACE total water
965 storage changes for China's Yangtze River Basin, *Remote Sens Environ*, 168, 177-193,
966 10.1016/j.rse.2015.07.003, 2015.

967 Masaki, Y., Hanasaki, N., Takahashi, K., and Hijioaka, Y.: Consequences of implementing a reservoir
968 operation algorithm in a global hydrological model under multiple meteorological forcing,
969 *Hydrological Sciences Journal*, 63, 1047-1061, 10.1080/02626667.2018.1473872, 2018a.

970 Masaki, Y., Hanasaki, N., Takahashi, K., and Hijioaka, Y.: Consequences of implementing a reservoir
971 operation algorithm in a global hydrological model under multiple meteorological forcing,
972 *Hydrolog Sci J*, 63, 1047-1061, 10.1080/02626667.2018.1473872, 2018b.

973 Mekonnen, M. M., and Hoekstra, A. Y.: Four billion people facing severe water scarcity, *Sci Adv*, 2,
974 10.1126/sciadv.1500323, 2016.

975 Mo, K. C.: Model-Based Drought Indices over the United States, *J Hydrometeorol*, 9, 1212-1230,
976 10.1175/2008jhm1002.1, 2008.

977 Myneni, R. B., Nemani, R. R., and Running, S. W.: Estimation of global leaf area index and absorbed
978 par using radiative transfer models, *Ieee T Geosci Remote*, 35, 1380-1393, 10.1109/36.649788,
979 1997.

980 Nazemi, A., and Wheeler, H. S.: On inclusion of water resource management in Earth system models -
981 Part 2: Representation of water supply and allocation and opportunities for improved modeling,
982 *Hydrol Earth Syst Sc*, 19, 63-90, 10.5194/hess-19-63-2015, 2015a.

983 Nazemi, A., and Wheeler, H. S.: On inclusion of water resource management in Earth system models -
984 Part 1: Problem definition and representation of water demand, *Hydrol Earth Syst Sc*, 19, 33-61,
985 10.5194/hess-19-33-2015, 2015b.

986 Nijssen, B., Lettenmaier, D. P., Liang, X., Wetzel, S. W., and Wood, E. F.: Streamflow simulation for
987 continental-scale river basins, *Water Resour Res*, 33, 711-724, 10.1029/96wr03517, 1997.

988 Nijssen, B., O'Donnell, G. M., Hamlet, A. F., and Lettenmaier, D. P.: Hydrologic sensitivity of global
989 rivers to climate change, *Climatic Change*, 50, 143-175, 10.1023/A:1010616428763, 2001a.

990 Nijssen, B., O'Donnell, G. M., Lettenmaier, D. P., Lohmann, D., and Wood, E. F.: Predicting the
991 discharge of global rivers, *J Climate*, 14, 3307-3323, 10.1175/1520-
992 0442(2001)014<3307:Ptdogr>2.0.Co;2, 2001b.

993 Nijssen, B., Schnur, R., and Lettenmaier, D. P.: Global retrospective estimation of soil moisture using
994 the variable infiltration capacity land surface model, 1980-93, *J Climate*, 14, 1790-1808,
995 10.1175/1520-0442(2001)014<1790:Greosm>2.0.Co;2, 2001c.

996 Nilsson, C., Reidy, C. A., Dynesius, M., and Revenga, C.: Fragmentation and flow regulation of the
997 world's large river systems, *Science*, 308, 405-408, 10.1126/science.1107887, 2005.

998 Oki, T., Musiak, K., Matsuyama, H., and Masuda, K.: Global Atmospheric Water-Balance and Runoff
999 from Large River Basins, *Hydrol Process*, 9, 655-678, 10.1002/hyp.3360090513, 1995.

1000 Oki, T., and Kanae, S.: Global hydrological cycles and world water resources, *Science*, 313, 1068-1072,
1001 10.1126/science.1128845, 2006.

1002 Pastor, A. V., Ludwig, F., Biemans, H., Hoff, H., and Kabat, P.: Accounting for environmental flow
1003 requirements in global water assessments, *Hydrol Earth Syst Sc*, 18, 5041-5059, 10.5194/hess-
1004 18-5041-2014, 2014.

1005 Pastor, A. V., Palazzo, A., Havlik, P., Biemans, H., Wada, Y., Obersteiner, M., Kabat, P., and Ludwig,
1006 F.: The global nexus of food–trade–water sustaining environmental flows by 2050, *Nature*
1007 *Sustainability*, 2, 499-507, 10.1038/s41893-019-0287-1, 2019.

1008 Poff, N. L., Richter, B. D., Arthington, A. H., Bunn, S. E., Naiman, R. J., Kendy, E., Acreman, M.,
1009 Apse, C., Bledsoe, B. P., Freeman, M. C., Henriksen, J., Jacobson, R. B., Kennen, J. G., Merritt,
1010 D. M., O'Keeffe, J. H., Olden, J. D., Rogers, K., Tharme, R. E., and Warner, A.: The ecological
1011 limits of hydrologic alteration (ELOHA): a new framework for developing regional
1012 environmental flow standards, *Freshwater Biol*, 55, 147-170, 10.1111/j.1365-
1013 2427.2009.02204.x, 2010.

1014 Pokhrel, Y., Hanasaki, N., Koirala, S., Cho, J., Yeh, P. J.-F., Kim, H., Kanae, S., and Oki, T.:
1015 Incorporating Anthropogenic Water Regulation Modules into a Land Surface Model, *J*
1016 *Hydrometeorol*, 13, 255-269, 10.1175/jhm-d-11-013.1, 2012a.

1017 Pokhrel, Y., Hanasaki, N., Koirala, S., Cho, J., Yeh, P. J. F., Kim, H., Kanae, S., and Oki, T.:
1018 Incorporating Anthropogenic Water Regulation Modules into a Land Surface Model, *J*
1019 *Hydrometeorol*, 13, 255-269, 10.1175/Jhm-D-11-013.1, 2012b.

1020 Pokhrel, Y. N., Koirala, S., Yeh, P. J.-F., Hanasaki, N., Longuevergne, L., Kanae, S., and Oki, T.:
1021 Incorporation of groundwater pumping in a global Land Surface Model with the representation
1022 of human impacts, *Water Resour Res*, 51, 78-96, 10.1002/2014wr015602, 2015.

1023 Pokhrel, Y. N., Hanasaki, N., Wada, Y., and Kim, H.: Recent progresses in incorporating human land-
1024 water management into global land surface models toward their integration into Earth system
1025 models, *Wires Water*, 3, 548-574, 10.1002/wat2.1150, 2016.

1026 Portmann, F. T., Siebert, S., and Döll, P.: MIRCA2000-Global monthly irrigated and rainfed crop areas
1027 around the year 2000: A new high-resolution data set for agricultural and hydrological modeling,
1028 *Global Biogeochem Cy*, 24, 10.1029/2008gb003435, 2010.

1029 Postel, S. L., Daily, G. C., and Ehrlich, P. R.: Human appropriation of renewable fresh water, *Science*,
1030 271, 785-788, 10.1126/science.271.5250.785, 1996.

- 1031 Reed, B., and Reed, B.: How much water is needed in emergencies, Water, Engineering and
1032 Development Centre, Leicestershire, 2013.
- 1033 Richter, B. D., Davis, M. M., Apse, C., and Konrad, C.: A Presumptive Standard for Environmental
1034 Flow Protection, *River Res Appl*, 28, 1312-1321, 10.1002/rra.1511, 2012.
- 1035 Rodell, M., Velicogna, I., and Famiglietti, J. S.: Satellite-based estimates of groundwater depletion in
1036 India, *Nature*, 460, 999-U980, 10.1038/nature08238, 2009.
- 1037 Roman, M. O., Wang, Z. S., Sun, Q. S., Kalb, V., Miller, S. D., Molthan, A., Schultz, L., Bell, J., Stokes,
1038 E. C., Pandey, B., Seto, K. C., Hall, D., Oda, T., Wolfe, R. E., Lin, G., Golpayegani, N.,
1039 Devadiga, S., Davidson, C., Sarkar, S., Praderas, C., Schmaltz, J., Boller, R., Stevens, J.,
1040 Gonzalez, O. M. R., Padilla, E., Alonso, J., Detres, Y., Armstrong, R., Miranda, I., Conte, Y.,
1041 Marrero, N., MacManus, K., Esch, T., and Masuoka, E. J.: NASA's Black Marble nighttime
1042 lights product suite, *Remote Sens Environ*, 210, 113-143, 10.1016/j.rse.2018.03.017, 2018.
- 1043 Rost, S., Gerten, D., Bondeau, A., Lucht, W., Rohwer, J., and Schaphoff, S.: Agricultural green and blue
1044 water consumption and its influence on the global water system, *Water Resour Res*, 44,
1045 10.1029/2007wr006331, 2008.
- 1046 Rougé, C., Reed, P. M., Grogan, D. S., Zuidema, S., Prusevich, A., Glidden, S., Lamontagne, J. R., and
1047 Lammers, R. B.: Coordination and Control: Limits in Standard Representations of Multi-
1048 Reservoir Operations in Hydrological Modeling, *Hydrol. Earth Syst. Sci. Discuss.*, 2019, 1-37,
1049 10.5194/hess-2019-589, 2019.
- 1050 Sellers, P. J., Tucker, C. J., Collatz, G. J., Los, S. O., Justice, C. O., Dazlich, D. A., and Randall, D. A.:
1051 A Global 1-Degrees-by-1-Degrees Ndvi Data Set for Climate Studies .2. The Generation of
1052 Global Fields of Terrestrial Biophysical Parameters from the Ndvi, *Int J Remote Sens*, 15, 3519-
1053 3545, 10.1080/01431169408954343, 1994.
- 1054 Shiklomanov, I. A.: Appraisal and assessment of world water resources, *Water Int*, 25, 11-32, Doi
1055 10.1080/02508060008686794, 2000.
- 1056 Shuttleworth, W. J.: Evaporation, in: *Handbook of hydrology*, edited by: Maidment, D. R., McGraw-
1057 Hill, New York, 53, 1993.
- 1058 Smakhtin, V., Revenga, C., and Döll, P.: A pilot global assessment of environmental water requirements
1059 and scarcity, *Water Int*, 29, 307-317, 10.1080/02508060408691785, 2004.
- 1060 Smith, M.: CROPWAT: A computer program for irrigation planning and managemetn, Food and
1061 Agricultural Organisation, Rome, Italy, 127, 1996.
- 1062 Steinfeld, H., Gerber, P., Wassenaar, T. D., Castel, V., Rosales, M., and De Haan, C.: Livestock's long
1063 shadow: environmental issues and options, Food and Agricultural Organisation, Rome, Italy,
1064 416 pp., 2006.
- 1065 Sutanudjaja, E. H., van Beek, R., Wanders, N., Wada, Y., Bosmans, J. H. C., Drost, N., van der Ent, R.
1066 J., de Graarf, I. E. M., Hoch, J. M., de Jong, K., Karssenber, D., Lopez, P. L., Pessenteiner, S.,

1067 Schmitz, O., Straatsma, M. W., Vannamettee, E., Wisser, D., and Bierkens, M. F. P.: PCR-
1068 GLOBWB 2: a 5 arcmin global hydrological and water resources model, *Geosci Model Dev*, 11,
1069 2429-2453, 10.5194/gmd-11-2429-2018, 2018.

1070 Takata, K., Emori, S., and Watanabe, T.: Development of the minimal advanced treatments of surface
1071 interaction and runoff, *Global Planet Change*, 38, 209-222, 10.1016/S0921-8181(03)00030-4,
1072 2003.

1073 Tessler, Z. D., Vorosmarty, C. J., Grossberg, M., Gladkova, I., Aizenman, H., Syvitski, J. P. M., and
1074 Foufoula-Georgiou, E.: Profiling risk and sustainability in coastal deltas of the world, *Science*,
1075 349, 638-643, 10.1126/science.aab3574, 2015.

1076 Turner, S. W. D., Hejazi, M., Yonkofski, C., Kim, S. H., and Kyle, P.: Influence of Groundwater
1077 Extraction Costs and Resource Depletion Limits on Simulated Global Nonrenewable Water
1078 Withdrawals Over the Twenty-First Century, *Earth's Future*, 7, 123-135,
1079 10.1029/2018ef001105, 2019.

1080 Van Beek, L. P. H., and Bierkens, M. F. P.: The global hydrological model PCR-GLOBWB:
1081 conceptualization, parameterization and verification, *Departement of physical geography*,
1082 Utrecht university, Utrecht, The Netherlands, 53, 2008.

1083 van Vliet, M. T. H., Wiberg, D., Leduc, S., and Riahi, K.: Power-generation system vulnerability and
1084 adaptation to changes in climate and water resources, *Nat Clim Change*, 6, 375-+,
1085 10.1038/Nclimate2903, 2016.

1086 Vassolo, S., and Döll, P.: Global-scale gridded estimates of thermoelectric power and manufacturing
1087 water use, *Water Resour Res*, 41, 10.1029/2004wr003360, 2005.

1088 Voisin, N., Li, H., Ward, D., Huang, M., Wigmosta, M., and Leung, L. R.: On an improved sub-regional
1089 water resources management representation for integration into earth system models, *Hydrol
1090 Earth Syst Sc*, 17, 3605-3622, 10.5194/hess-17-3605-2013, 2013.

1091 Voisin, N., Hejazi, M. I., Leung, L. R., Liu, L., Huang, M. Y., Li, H. Y., and Tesfa, T.: Effects of
1092 spatially distributed sectoral water management on the redistribution of water resources in an
1093 integrated water model, *Water Resour Res*, 53, 4253-4270, 10.1002/2016wr019767, 2017.

1094 Voisin, N., Kintner-Meyer, M., Wu, D., Skaggs, R., Fu, T., Zhou, T., Nguyen, T., and Kraucunas, I.:
1095 OPPORTUNITIES FOR JOINT WATER-ENERGY MANAGEMENT Sensitivity of the 2010
1096 Western US Electricity Grid Operations to Climate Oscillations, *B Am Meteorol Soc*, 99, 299-
1097 312, 10.1175/Bams-D-16-0253.1, 2018.

1098 Vorosmarty, C. J., McIntyre, P. B., Gessner, M. O., Dudgeon, D., Prusevich, A., Green, P., Glidden, S.,
1099 Bunn, S. E., Sullivan, C. A., Liermann, C. R., and Davies, P. M.: Global threats to human water
1100 security and river biodiversity, *Nature*, 467, 555-561, 10.1038/nature09440, 2010.

1101 Voß, F., and Flörke, M.: Spatially explicit estimates of past and present manufacturing and energy water
1102 use, *Center for environmental systems research*, Kassel, 17, 2010.

1103 Wada, Y., van Beek, L. P. H., and Bierkens, M. F. P.: Modelling global water stress of the recent past:
1104 on the relative importance of trends in water demand and climate variability, *Hydrol Earth Syst*
1105 *Sc*, 15, 3785-3808, 10.5194/hess-15-3785-2011, 2011a.

1106 Wada, Y., van Beek, L. P. H., Viviroli, D., Durr, H. H., Weingartner, R., and Bierkens, M. F. P.: Global
1107 monthly water stress: 2. Water demand and severity of water stress, *Water Resour Res*, 47,
1108 10.1029/2010wr009792, 2011b.

1109 Wada, Y., and Bierkens, M. F. P.: Sustainability of global water use: past reconstruction and future
1110 projections, *Environ Res Lett*, 9, 104003, 10.1088/1748-9326/9/10/104003, 2014.

1111 Wada, Y., Wisser, D., and Bierkens, M. F. P.: Global modeling of withdrawal, allocation and
1112 consumptive use of surface water and groundwater resources, *Earth Syst Dynam*, 5, 15-40,
1113 10.5194/esd-5-15-2014, 2014.

1114 Weedon, G. P., Balsamo, G., Bellouin, N., Gomes, S., Best, M. J., and Viterbo, P.: The WFDEI
1115 meteorological forcing data set: WATCH Forcing Data methodology applied to ERA-Interim
1116 reanalysis data, *Water Resour Res*, 50, 7505-7514, 10.1002/2014wr015638, 2014.

1117 Wisser, D., Fekete, B. M., Vorosmarty, C. J., and Schumann, A. H.: Reconstructing 20th century global
1118 hydrography: a contribution to the Global Terrestrial Network- Hydrology (GTN-H), *Hydrol*
1119 *Earth Syst Sc*, 14, 1-24, 10.5194/hess-14-1-2010, 2010a.

1120 Wisser, D., Fekete, B. M., Vörösmarty, C. J., and Schumann, A. H.: Reconstructing 20th century global
1121 hydrography: a contribution to the Global Terrestrial Network- Hydrology (GTN-H), *Hydrol.*
1122 *Earth Syst. Sci.*, 14, 1-24, 10.5194/hess-14-1-2010, 2010b.

1123 Wood, A. W., and Lettenmaier, D. P.: A test bed for new seasonal hydrologic forecasting approaches in
1124 the western United States, *B Am Meteorol Soc*, 87, 1699-+, 10.1175/Bams-87-12-1699, 2006.

1125 Yassin, F., Razavi, S., Elshamy, M., Davison, B., Sapriza-Azuri, G., and Wheeler, H.: Representation
1126 and improved parameterization of reservoir operation in hydrological and land-surface models,
1127 *Hydrol. Earth Syst. Sci.*, 23, 3735-3764, 10.5194/hess-23-3735-2019, 2019.

1128 Zhao, G., Gao, H. L., Naz, B. S., Kao, S. C., and Voisin, N.: Integrating a reservoir regulation scheme
1129 into a spatially distributed hydrological model, *Adv Water Resour*, 98, 16-31,
1130 10.1016/j.advwatres.2016.10.014, 2016.

1131 Zhou, T., Haddeland, I., Nijssen, B., and Lettenmaier, D. P.: Human induced changes in the global water
1132 cycle, *AGU Geophysical Monograph Series*, Submitted, 2015.

1133 Zhou, T., Nijssen, B., Gao, H. L., and Lettenmaier, D. P.: The Contribution of Reservoirs to Global
1134 Land Surface Water Storage Variations, *J Hydrometeorol*, 17, 309-325, 10.1175/Jhm-D-15-
1135 0002.1, 2016.

1136 Zhou, T., Voisin, N., Leng, G. Y., Huang, M. Y., and Kraucunas, I.: Sensitivity of Regulated Flow
1137 Regimes to Climate Change in the Western United States, *J Hydrometeorol*, 19, 499-515,
1138 10.1175/Jhm-D-17-0095.1, 2018.

1139 Zhu, C. M., Leung, L. R., Gochis, D., Qian, Y., and Lettenmaier, D. P.: Evaluating the Influence of
1140 Antecedent Soil Moisture on Variability of the North American Monsoon Precipitation in the
1141 Coupled MM5/VIC Modeling System, *J Adv Model Earth Sy*, 1, 10.3894/James.2009.1.13,
1142 2009.
1143